UNCLASSIFIED

AD NUMBER

AD245560

NEW LIMITATION CHANGE

TO

Approved for public release, distribution unlimited

FROM

Distribution: Further dissemination only as directed by Naval Ordnance Systems Command, Washington DC; 14 Jan 1960 or higher DoD authority.

AUTHORITY

USNOL ltr, 29 Aug 1974

THIS PAGE IS UNCLASSIFIED

NAVY FILE NAVORD Report 4516

NTIS

AD-245560

NAVORD REPORT 4516

[redacted]

DYNAMIC AND STATIC STABILITY MEASUREMENTS OF THE BASIC FINNER AT SUPERSONIC SPEEDS (U)

14 JANUARY 1960

U. S. NAVAL ORDNANCE LABORATORY
WHITE OAK, MARYLAND

NAVORD Report 4516

Aerodynamics Research Report 390

DYNAMIC AND STATIC STABILITY MEASUREMENTS OF THE BASIC FINNER AT SUPERSONIC SPEEDS

Prepared by:

Irving Shantz
Robert T. Groves

ABSTRACT: Dynamic stability data in the form of damping force and moment coefficients were obtained in the NOL Supersonic Tunnel No. 1. These measurements were made in the Mach number range 1.58 through 3.24. Static stability data in the form of normal force and pitching moment coefficients were determined in the Mach number range 1.58 through 3.86. Both dynamic and static stability coefficients are compared with free flight results obtained in the NOL and BRL ballistics firing ranges.

PUBLISHED SEPTEMBER 1960

Dynamic and static stability data were obtained at supersonic speeds for the ten caliber basic finner. This investigation was performed for RRRE-7 of the Bureau of Naval Weapons under Task Number 803-717/73001/03073.

JOHN A. QUENSE', Acting
Captain, USN
Commander

R. KENNETH LOBB
By direction

CONTENTS

ILLUSTRATIONS

DYNAMIC AND STATIC STABILITY MEASUREMENTS OF THE BASIC FINNER AT SUPERSONIC SPEEDS

INTRODUCTION

1. Basic Finner is the name given to a standard configuration that has been selected for use in checking various test techniques and new instrumentation. An attempt has been made to obtain all the important aerodynamic coefficients for this shape. New test techniques can thus be evaluated by comparing the results obtained using the techniques or instrumentation with previously obtained data.

2. Results from two separate wind-tunnel investigations are presented in this report. These investigations are, static stability measurements up to large angles of attack and dynamic stability damping measurements up to large amplitudes of oscillation. The static stability investigation was conducted to provide supplementary large angle of attack data to the existing small angle values. The damping investigation was conducted to provide large amplitude damping values and to validate the freely oscillating model method used to make these measurements.

3. From the static stability tests normal force and pitching moment coefficients and center of pressure locations were obtained. The dynamic stability damping tests yielded damping moment and damping force coefficients. Measurements were made at each of two center of mass locations. Normal force and pitching moment coefficients were also obtained from the damping tests. Correlative comparisons are made with corresponding Ballistics Range values. Damping moment coefficients are also compared with similar wind-tunnel values obtained employing a small amplitude damping balance. These wind-tunnel investigations were performed at supersonic speeds; the Mach number ranges were 1.58 through 3.24 for the damping tests and 1.58 through 3.86 for the static tests.

SYMBOLS

Free-stream parameters:

M	Mach number
V	free-stream velocity (ft/sec)
ρ	free-stream density (slugs/ft^3)
$\bar{q}$	free-stream dynamic pressure (psfa) = $1/2\ \rho V^2$

Model attitude parameters:

α	angular amplitude (damping tests)(radians or deg)

α	angle of attack (static tests)(deg)
$\dot{\alpha}$	angular velocity (radians/sec)
$\ddot{\alpha}$	angular acceleration (radians/sec^2)
ϕ	angle of roll (deg)
q	transverse angular velocity

<u>Model reference dimensions:</u>

D	body diameter = 1 caliber
S	body cross-sectional arer = $\pi D^2/4$ (ft^2)
I	transverse moment of inertia (slugs ft^2)
t	time (sec)
x	axial station location (calibers)(x = 0 at base of cylinder)

<u>Aerodynamic forces, moments and coefficients:</u>

F_N	normal force (lbs)
$F_{N_q}(q) + F_{N_{\dot{\alpha}}}(\dot{\alpha})$	total damping force (lbs)
M	pitching or restoring moment (ft-lbs)
M_α	pitching or restoring moment slope (ft-lbs/rad)
$M_q(q)+M_{\dot{\alpha}}(\dot{\alpha})$	total damping moment (ft-lbs)
C_N	normal force coefficient = $F_N/\bar{q}S$
C_{N_α}	normal force coefficient per radian
$(C_{N_q} + C_{N_{\dot{\alpha}}})$	total damping force coefficient
C_M	pitching or restoring moment coefficient = $M/\bar{q}SD$
C_{M_α}	pitching or restoring moment coefficient slope
$(C_{M_q} + C_{M_{\dot{\alpha}}})$	total damping moment coefficient
C.P.	center of pressure (calibers from nose)

Subscripts or Sub-subscripts:

o	initial conditions
p	peak amplitude conditions
1,2,3,---n	events or measurements in sequence of time or station location (positive for stations forward of base)

DESCRIPTION OF MODELS

4. The aerodynamic configuration used in these tests is usually referred to as the Basic Finner. Basically it is a cone-cylinder with four rectangular fins and is ten calibers in overall length. This configuration is diagrammatically shown in Figure 1. Three different size models were employed. These model sizes were dictated by the individual requirements of each test technique. The small amplitude damping balance model diameter (D) was 1.870 inches; the large amplitude damping model diameter was 1.500 inches; the static force and moment model diameter was 1.000 inch.

TEST TECHNIQUES

5. Although damping measurements made with the small-amplitude sting mount balance have been reported in a previous publication, consistent reference is made to these results in this report. Therefore, a brief description of this balance method is included as background information for data comparisons made in discussing test results. The small amplitude damping balance consists of a stiff sting, a strain-gage flexure at the model end of the sting, and a tripping device to set the model in motion. A sketch of the balance is shown in Figure 1A and it is described in detail in reference (a). The balance method yields damping moment data in the pitch plane for oscillatory motions of approximately plus and minus two degrees about the trim attitude, which is $\alpha = 0^{o}$ for these tests. This balance can measure the damping moment of statically unstable as well as statically stable configurations. The small amplitude damping balance method is a free decay technique in that no additional energy is fed into the system after the initial angular displacement has been accomplished and the model is released.

6. The freely oscillating model method yields damping data for oscillatory motions of up to plus and minus ninety degrees amplitude and like the small amplitude damping method is a free decay technique. Only statically stable models can be tested with this method. The free oscillation method consists of allowing a model to seek its trim attitude after it has been displaced from the trim attitude. Suspension of the model is mechanically accomplished by passing a shaft through the center of gravity of the model. This shaft is fastened to the model

structure by means of two very low friction instrument-type bearings which are contained within the model. Thus, the model is constrained to execute angular motion, about its rigidly held center of gravity, in one plane only. A photograph of this set-up is shown in Figure 1B. After the model has been displaced from its trim attitude and released, the motion of the model as it seeks its trim attitude is photographically recorded with a high-speed motion picture camera. A plot of the instantaneous angular attitude as a function of time is thus obtained and the resultant curve takes the form of damped periodic motion. This method yields a record of the motion of the model over large angular amplitudes. The equation of angular motion in one degree of freedom can be expressed as:

$$I\ddot{\alpha} + \mu\dot{\alpha} + M_{\alpha}\alpha = 0 \tag{1}$$

where:

I = moment of inertia

μ = damping constant

M_{α} = restoring or pitching moment slope

The damping moment coefficient is computed by the following equation in which (α) has been replaced by the peak angular amplitude (α_p) of any half cycle.

$$C_{M_q} + C_{M_{\dot{\alpha}}} = \frac{16}{\pi}\left(\frac{2I}{\rho V D^4}\right)\left[\frac{\ln\left({}^{\alpha}p/{}^{\alpha}p_o\right)}{t_p - t_{p_o}}\right] \tag{2}$$

where subscripts: p_o denotes initial peak amplitude conditions

p denotes peak amplitude conditions at some later time.

The restoring or pitching moment coefficient slope can be computed by the following equation:

$$C_{M_{\alpha}} = -\frac{2I}{\rho V^2 SD}\left\{\omega^2 + \left[\frac{\ln\left({}^{\alpha}p/{}^{\alpha}p_o\right)}{t_p - t_{p_o}}\right]^2\right\} \tag{3}$$

where: ω = circular frequency in radians per second.

The term $\left[\frac{\ln\left({}^{\alpha}p/{}^{\alpha}p_o\right)}{t_p - t_{p_o}}\right]^2$ is small in magnitude compared with ω^2; usually in the order of $0.01\,\omega^2$ and can be neglected.

7. The relationships expressed in equation (2) are valid only if the assumption of constancy of the coefficients in equation (1) is reasonably true. When the amplitude of the oscillatory motion becomes large, greater than plus and minus eight degrees, the assumption of constant coefficients in equation (1) is usually no longer reasonable. Applying the linear solution over the entire range of angular amplitudes no longer yields a univalue for the damping but yields results such as are shown below.

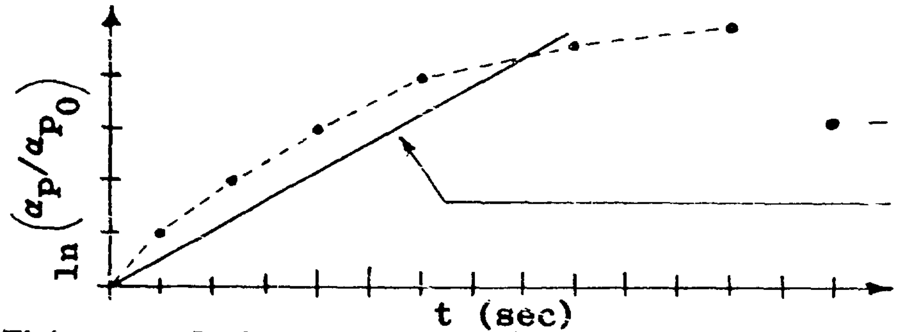

This precludes the use of the linear equation with constant coefficients to describe the motion over the entire range of amplitudes. This also indicated that the damping moment varied with angular attitude to the flow. Until more exact measurements of $\ddot{\alpha}$, $\dot{\alpha}$, and α can be made and substituted into a non-linear form of equation (1), approximate damping moment values for the larger angular amplitudes can be obtained by applying equation (2) in the following manner. The peak amplitudes and their respective times are tabulated or plotted as shown below.

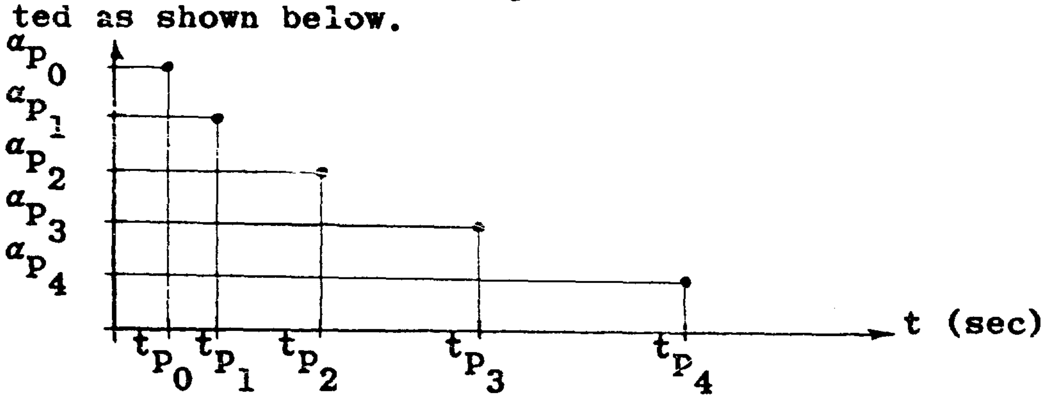

The damping moment coefficient is computed for discrete intervals of angular amplitudes: for example:

for the interval $\alpha_{p_o} \rightarrow \alpha_{p_1}$ or, average $\alpha_p = \dfrac{\alpha_{p_o} + \alpha_{p_1}}{2}$

$$\left(C_{M_q} + C_{M_{\dot{\alpha}}}\right)_1 = \frac{16}{\pi}\left(\frac{2I}{\rho V D^4}\right)\left[\frac{\ln\left(\alpha_{p_1}/\alpha_{p_o}\right)}{t_{p_1} - t_{p_o}}\right]$$

for the interval $\alpha_{p_1} \rightarrow \alpha_{p_2}$ or, average $\alpha_p = \frac{\alpha_{p_1} + \alpha_{p_2}}{2}$

$$(C_{M_q} + C_{M_{\dot{\alpha}}})_2 = \frac{16}{\pi} \left(\frac{2I}{\rho V D^4}\right) \left[\frac{\ln\left(\alpha_{p_2}/\alpha_{p_1}\right)}{t_{p_2} - t_{p_1}}\right]$$

Utilizing equation (2) in this fashion yields average damping moment coefficients which are a function of the average peak angular amplitudes.

DESCRIPTION OF THE FACILITY AND DISCUSSION OF TEST RESULTS

8. Aeroballistic Supersonic Tunnel No. 1 was used for all of the wind-tunnel tests reported herein. This tunnel operates as a blow-down facility and uses fixed block steel nozzles. Physical dimensions and operational specifications are given in detail in reference (b).

9. Static stability data in the form of normal force coefficients, pitching moment coefficients and centers of pressure are presented in Figures 2 through 15. These data were obtained using a standard internal strain-gage balance. This type of balance and the data reduction equations are described in detail in reference (c).

10. The dynamic or damping moment data are presented in Figures 16 through 22. In these figures the damping coefficients $(C_{M_q} + C_{M_{\dot{\alpha}}})$ are plotted against peak angular amplitude (α_p) for each Mach number. These data were obtained for a model roll attitude of $\phi = 45^{\circ}$ and for two center of gravity positions.

11. In order to make comparisons of these damping moment coefficients with those obtained from ballistics ranges only the small amplitude values could be used since the ballistics range results reproduced herein, reference (d), were obtained for small yaws only.

12. Comparisons of the damping moment coefficients with ballistics range results are presented in Figures 23 through 25. The damping moment coefficients $(C_{M_q} + C_{M_{\dot{\alpha}}})$ are plotted against Mach number in Figure 23 with center of gravity as parameter. Free-flight range results from reference (d) are also presented for comparison with the wind-tunnel data ob-

tained with the two measuring techniques. Damping moment coefficients obtained with the free-oscillation technique were arbitrarily selected for peak angular amplitudes of approximately 7.5 degrees. For the aerodynamic shape tested the damping is essentially constant with amplitude for oscillations from zero to eight degrees. Comparisons made with similar data obtained using the sting-mounted balance, for oscillatory amplitudes in the order of plus and minus two degrees, tend to confirm this assumption of constancy for this range of angular amplitudes.

13. Damping moment coefficients as a function of center of gravity position at Mach number 2.1 are presented in Figure 24. This type of plot better expresses the degree of agreement between coefficients obtained in the wind-tunnel test and the ballistics range. These wind-tunnel test data are compared with results obtained in the BRL and NOL range facilities. Mach number 2.1 was selected since it is in a region where most of the data exist. Comparisons at other Mach numbers show approximately the same results.

14. Damping force coefficients ($C_{N_q} + C_{N_{\dot{\alpha}}}$) calculated at the centroid of projected area, 6.39 calibers from the nose, are presented as a function of Mach number in Figure 25. These values were calculated using center of mass transformation equations. Considerable disagreement exists between these values and the results presented in reference (d). Deduction of the damping force coefficient ($C_{N_q} + C_{N_{\dot{\alpha}}}$) from the swerving motion of a projectile in free-flight is relatively difficult in that its contribution to the total swerving motion is small when compared with the static normal force (C_{N_α}) contribution. In most ballistics range experiments, the total swerving motion is held to a minimum to prevent drift of the projectile which could pull it out of the range of vision of the downrange photographic stations. At best, this direct method of determining damping force from the swerving motion resolves into a problem of measuring a small part of a small quantity. An alternate method of determining ($C_{N_q} + C_{N_{\dot{\alpha}}}$) utilizes the center of mass transformation relationships (see Appendix A). This involves a term containing the difference of two damping moments measured at two axial locations as well as the static components of the force and moment system. Since the term containing the difference between two damping moments is the major contributor, uncertainties of the order of ten to fifteen percent in determination of each damping moment value can lead to large errors in the determination of the damping force. Wind-tunnel uncertainty in the measurement of damping moments is of the order of plus or minus five percent for the type of shape used in these tests.

15. Pitching moment coefficients obtained from the free oscillation wind-tunnel test are compared with ballistics range results and with values obtained from a wind-tunnel static test; these comparisons are presented in Figures 26 through 28. Pitching moment coefficient slopes (C_{M_α}) presented in these comparisons were obtained for small angular amplitudes, of the order of plus and minus six degrees. These data are plotted against Mach number in Figure 25 with center of gravity position as the parameter. Figures 27 and 28 contain C_{M_α} plotted against center of gravity position at Mach numbers 1.8 and 2.1 respectively. Wind-tunnel dynamic and static stability coefficients presented for Mach numbers 1.8 and 2.1 were obtained by cross-plots of the particular coefficient with Mach number.

16. Normal force coefficient slopes (C_{N_α}) are plotted against Mach number in Figure 29. The free oscillation wind-tunnel data are compared with ballistics range results and static wind-tunnel values.

17. Center of pressure location is plotted against Mach number in Figure 30. Maximum spread of the data are of the order of three percent of total length.

18. Wind-tunnel free-stream parameters are presented in Appendix B. Reynolds numbers were computed using model axial length as the reference dimension.

CONCLUSIONS

19. From the various comparisons made of similar data obtained from two or more different sources employing dissimilar test techniques, close agreement of the various test results is in evidence with but one exception.

20. Damping moment coefficients obtained employing the freely oscillating model method are in agreement with small amplitude results obtained from the sting-mount balance wind-tunnel tests and ballistics range free-flight measurements. Lack of agreement with ballistics range values for the damping force coefficients cannot be explained as yet.

21. Static stability coefficients, obtained as a by-product of the free oscillation damping tests, are in reasonable agreement with static test wind-tunnel values and ballistics range free-flight measurements.

22. The freely oscillating model damping test technique is a valuable wind-tunnel research tool in that it is capable of measuring damping moments at large amplitudes of oscillatory motion. Close agreement of small amplitude values with other proven techniques strongly supports the validity of the large amplitude values. Refinements to the mechanics of this test technique are being developed at the present time. The highly non-linear character of the damping moment coefficient at large amplitudes of oscillation indicates the need for development of a more sophisticated equation of motion.

REFERENCES

(a) Shantz, I., "Small Amplitude Damping-in-Pitch Measurements in the NOL 40 x 40 cm Aeroballistics Wind Tunnels," NAVORD Report 3859, Conf., (1956)

(b) Meek, P. P., "Aeroballistic Research at the U. S. Naval Ordnance Laboratory," NOLR 1201, Unclass., (1956)

(c) Shantz, I., Gilbert, B. D., White, C. E., "NOL Wind-Tunnel Internal Strain-Gage Balance System," NAVORD Report 2972, Unclass., (1953)

(d) MacAllister, L. C., "The Aerodynamic Properties of a Simple Non Rolling Finned Cone-Cylinder Configuration Between Mach Numbers 1.0 and 2.5," Ballistic Research Laboratories Report No. 934.

(e) Murphy, C. H., Schmidt, L. E., "Effect of Length on the Aerodynamic Characteristics of Bodies-of-Revolution in Supersonic Flight," Ballistic Research Laboratories Report No. 876, Conf.

(f) Nicolaides, J. D., "On the Free-Flight Motions of Projectiles with Slight Configurational Asymmetry," Ballistic Research Laboratories Report No. 858.

(g) Nicolaides, J. D., "Variation of the Aerodynamic Force and Moment Coefficients with Reference System," Ballistic Research Laboratories Technical Note No. 746, (1952)

APPENDIX A

Center of Mass Transformation

Aerodynamic moment coefficients measured at two different axial locations can be related by moment transfer formulae (references (d), (e), (f), and (g)), according to the following relationships:

$$(C_{N_\alpha})_2 = (C_{N_\alpha})_1 \tag{1}$$

$$(C_{M_\alpha})_2 = (C_{M_\alpha})_1 + (X_2 - X_1)\, C_{N_\alpha} \tag{2}$$

$$(C_{N_q} + C_{N_{\dot\alpha}})_2 = (C_{N_q} + C_{N_{\dot\alpha}})_1 + 2(X_2 - X_1)\, C_{N_\alpha} \tag{3}$$

$$(C_{M_q} + C_{M_{\dot\alpha}})_2 = (C_{M_q} + C_{M_{\dot\alpha}})_1 - 2(X_2 - X_1)^2\, C_{N_\alpha} + (X_2 - X_1)\left[(C_{N_q} + C_{N_{\dot\alpha}})_1 + 2(C_{M_\alpha})_1\right] \tag{4}$$

$$(C_{N_q} + C_{N_{\dot\alpha}})_1 + 2(C_{M_\alpha})_1 = \frac{(C_{M_q} + C_{M_{\dot\alpha}})_2 - (C_{M_q} + C_{M_{\dot\alpha}})_1}{(X_2 - X_1)} + 2\left[(C_{M_\alpha})_2 - (C_{M_\alpha})_1\right]$$

$$(C_{N_q} + C_{N_{\dot\alpha}})_1 = \frac{(C_{M_q} + C_{M_{\dot\alpha}})_2 - (C_{M_q} + C_{M_{\dot\alpha}})_1}{(X_2 - X_1)} + 2\left[(C_{M_\alpha})_2 - 2(C_{M_\alpha})_1\right] \tag{5a}$$

or

$$(C_{N_q} + C_{N_{\dot\alpha}})_2 = \frac{(C_{M_q} + C_{M_{\dot\alpha}})_2 - (C_{M_q} + C_{M_{\dot\alpha}})_1}{(X_2 - X_1)} + 4\left[(C_{M_\alpha})_2 - \frac{3}{2}(C_{M_\alpha})_1\right] \tag{5b}$$

APPENDIX B

Free-Stream Conditions

Static Tests:

M	$\bar{q}$	Reynolds No. x 10^{-6} (A)
1.58	6.03	3.79
1.76	5.75	3.54
2.17	4.68	3.00
2.48	3.78	2.65
2.88	2.76	2.21
3.22	2.08	1.90

Dynamic Tests:

M	$\bar{q}$	ρV	Reynolds No. x 10^{-6} (B)
1.58	6.19	1.236	5.69
1.76	5.83	1.089	5.31
1.89	5.52	0.987	5.09
2.16	4.74	0.787	4.50
2.48	3.79	0.589	3.98
2.88	2.75	0.403	3.31
3.24	2.04	0.286	2.80

(A) Based on 10.00 inches overall length

(B) Based on 15.00 inches overall length

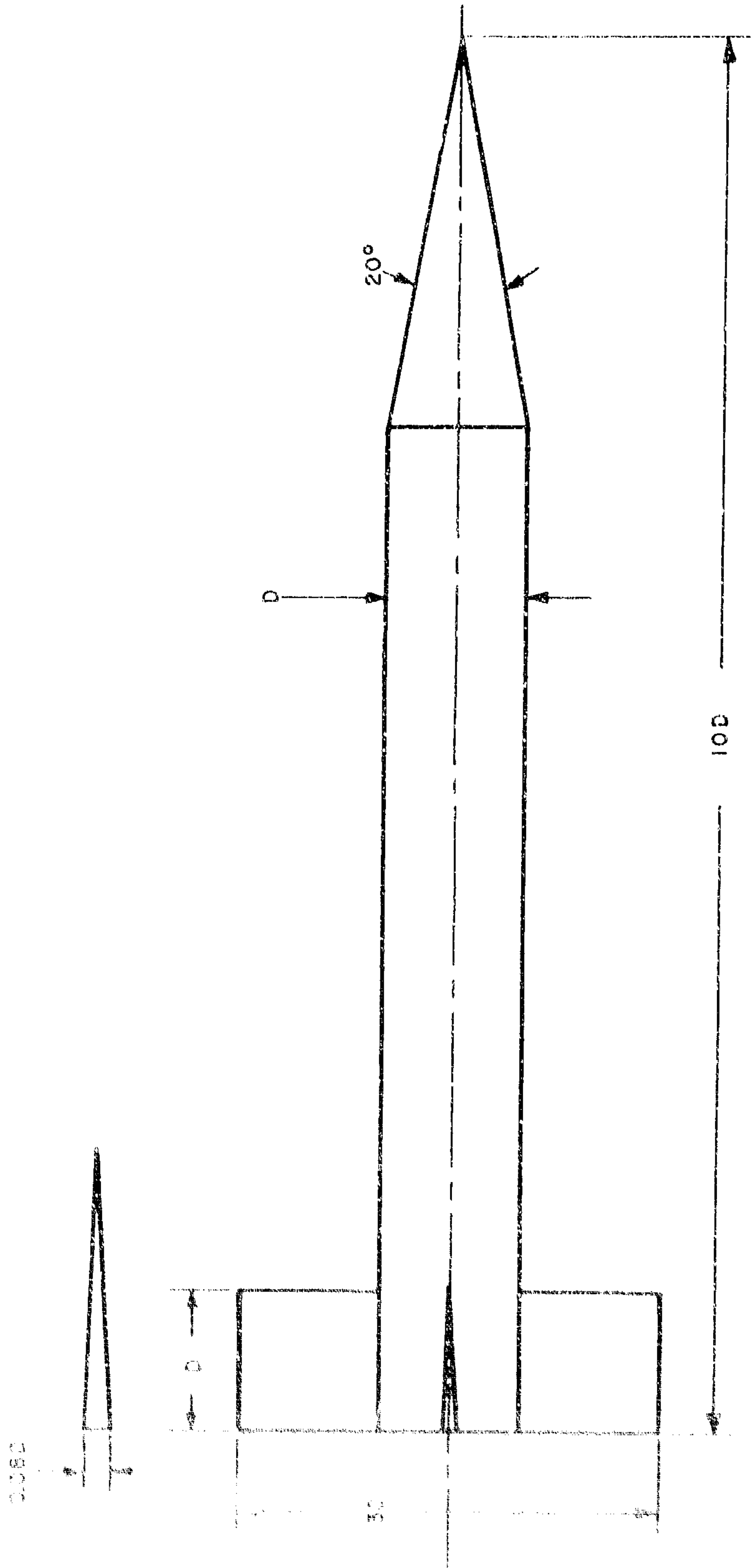

FIG. 1 BASIC FINNER

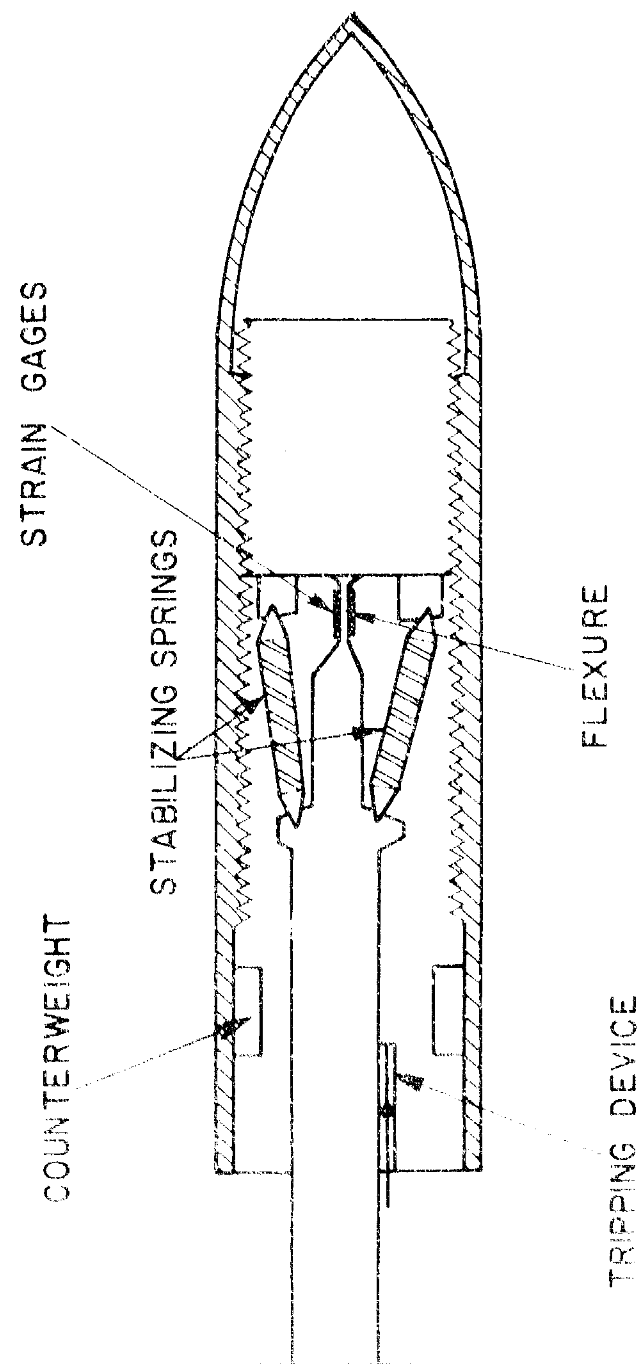

FIG. IA SCHEMATIC OF THE SMALL – AMPLITUDE DAMPING BALANCE

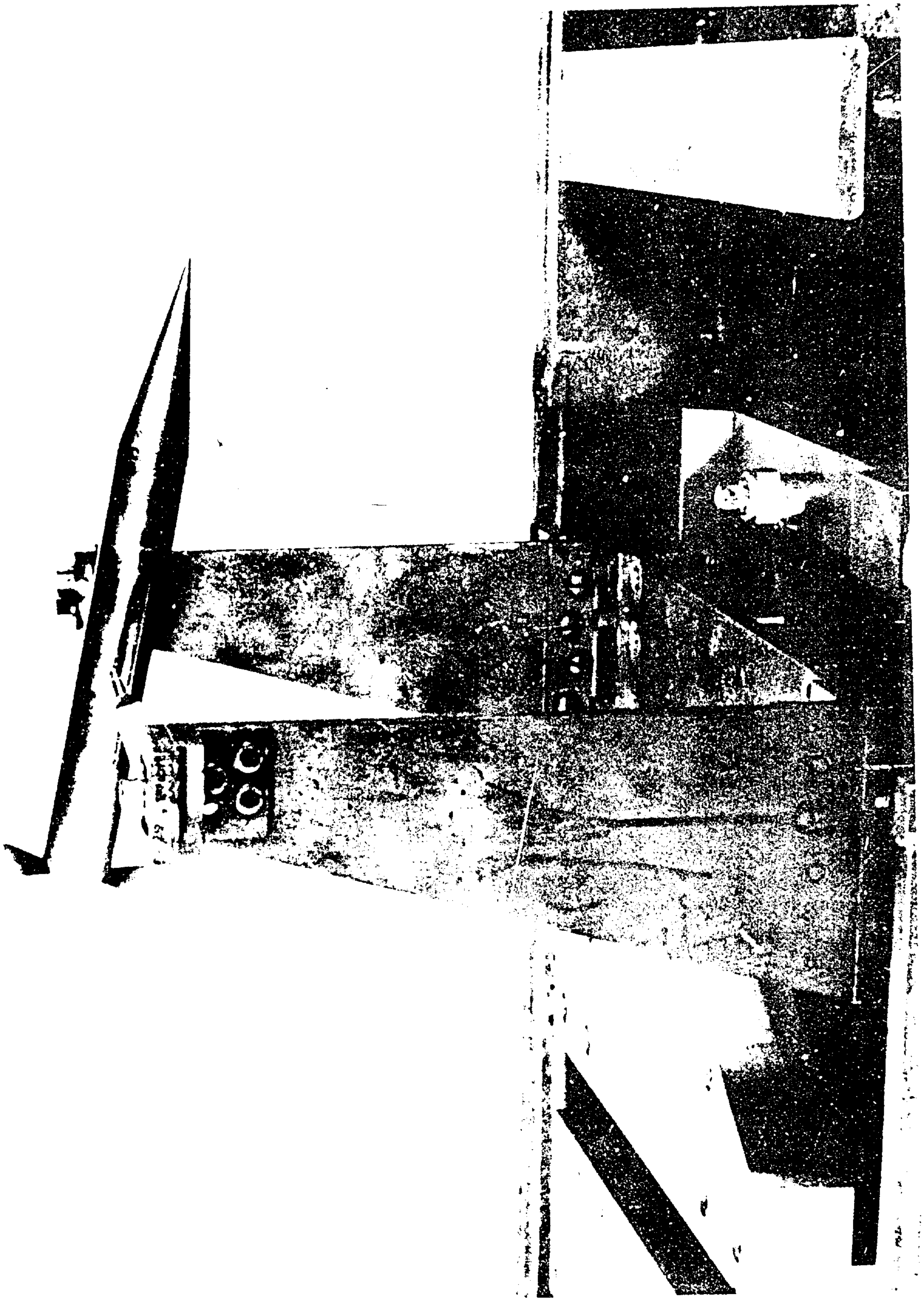

FIG. 1B BASIC FINNER MODEL — LARGE-AMPLITUDE DAMPING SUPPORT

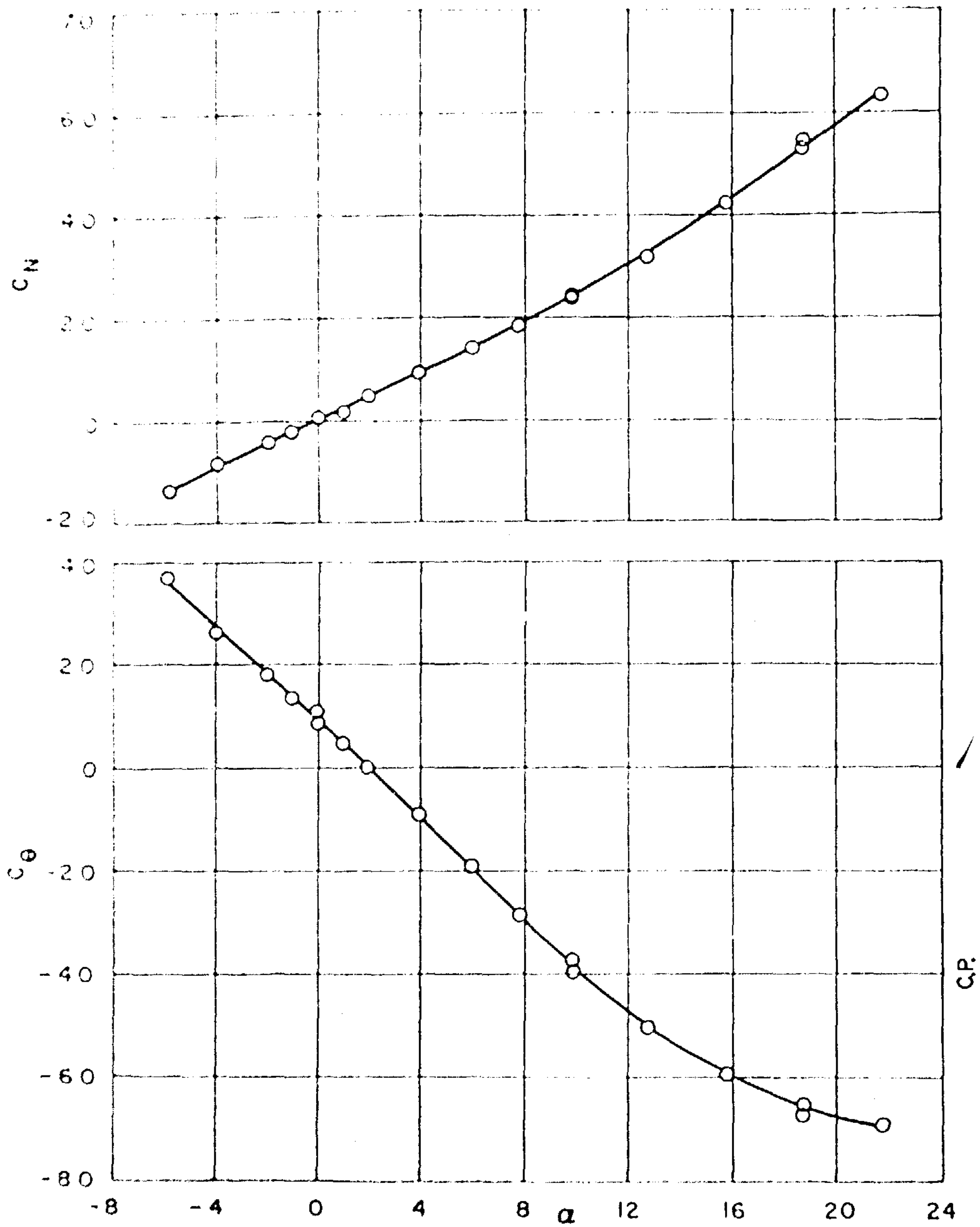

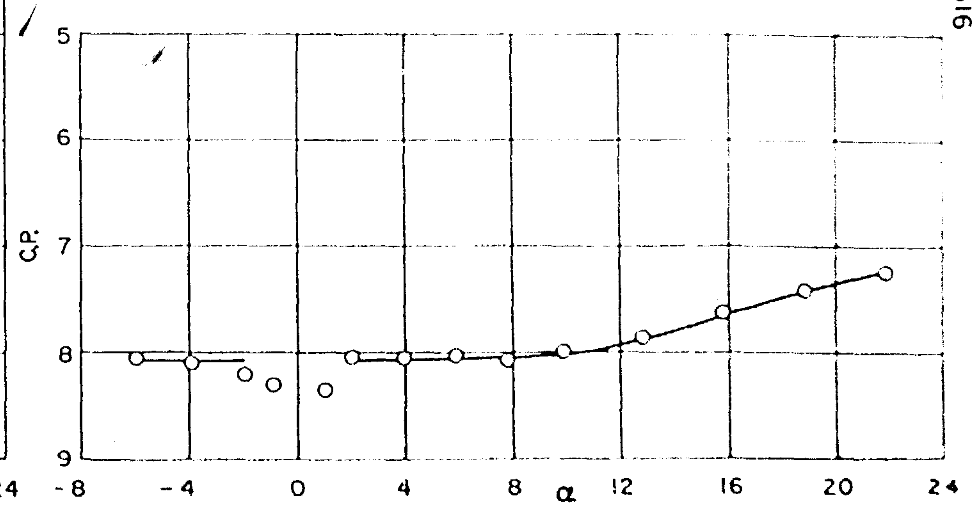

FIG. 2 BASIC FINNER
STATIC STABILITY
M=1.58 Ø=0°
C.G.=6 CALIBERS FROM NOSE

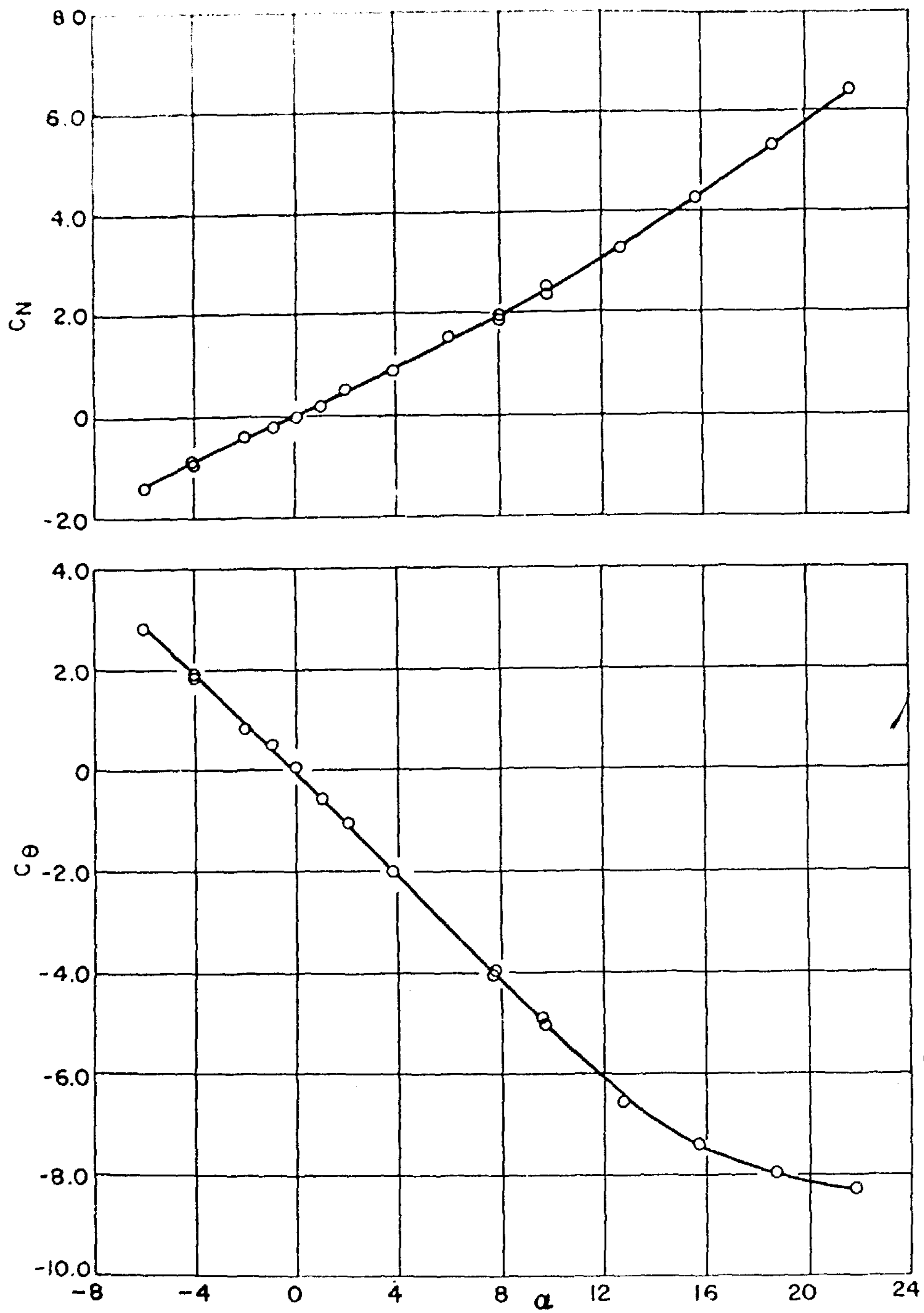

FIG. 3 BASIC FINNER
STATIC STABILITY
M=1.58 Ø=45°
C.G.=6 CALIBERS FROM NOSE

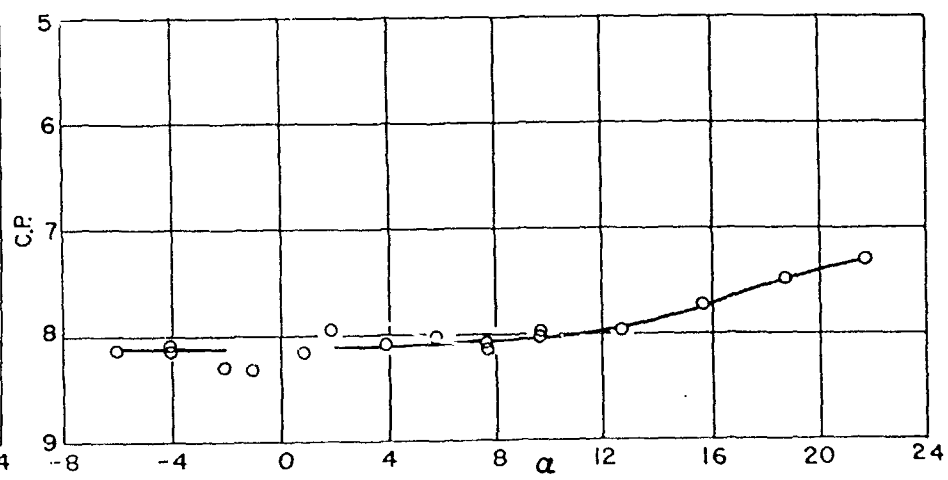

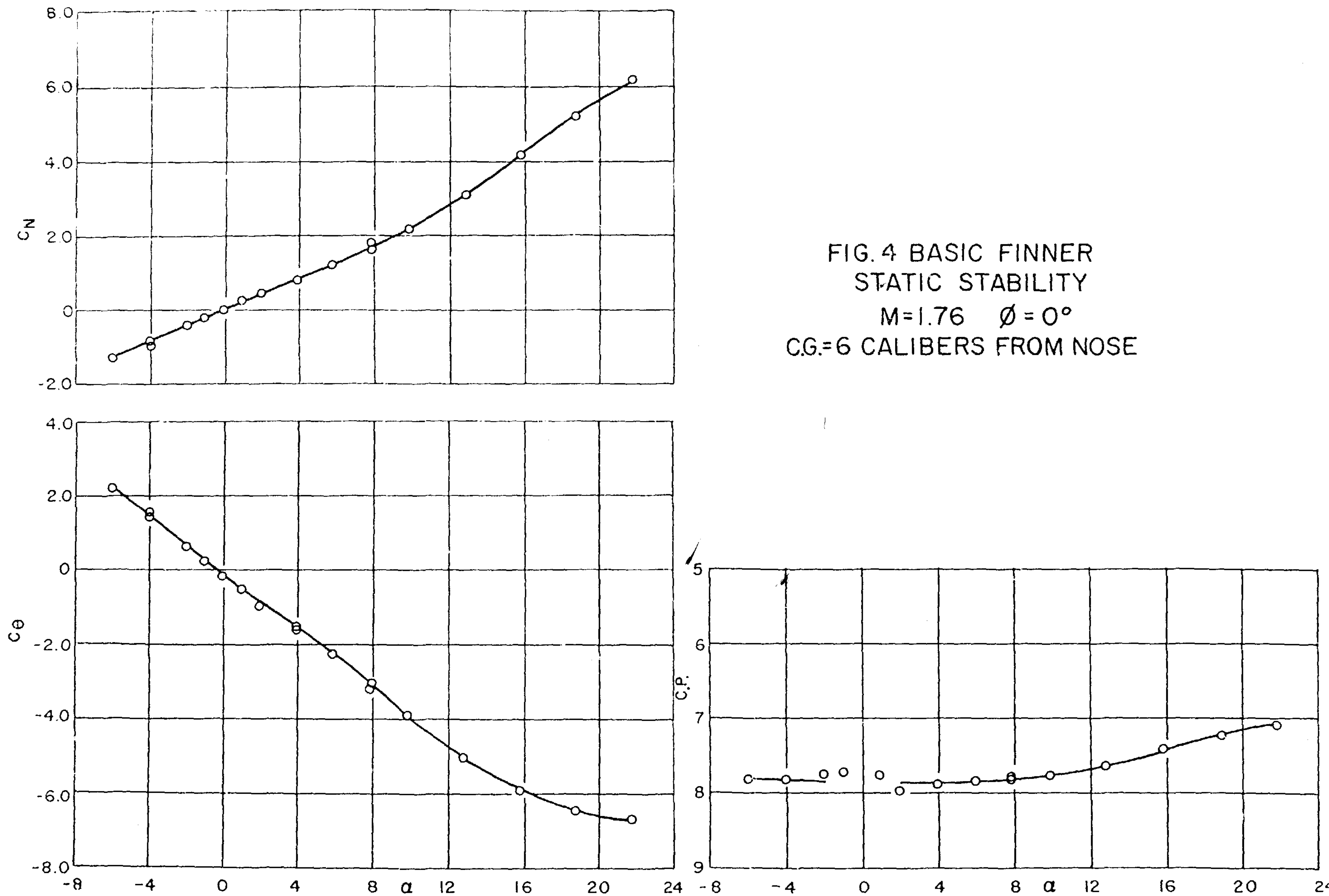

FIG. 4 BASIC FINNER
STATIC STABILITY
M=1.76 Ø=0°
C.G.=6 CALIBERS FROM NOSE

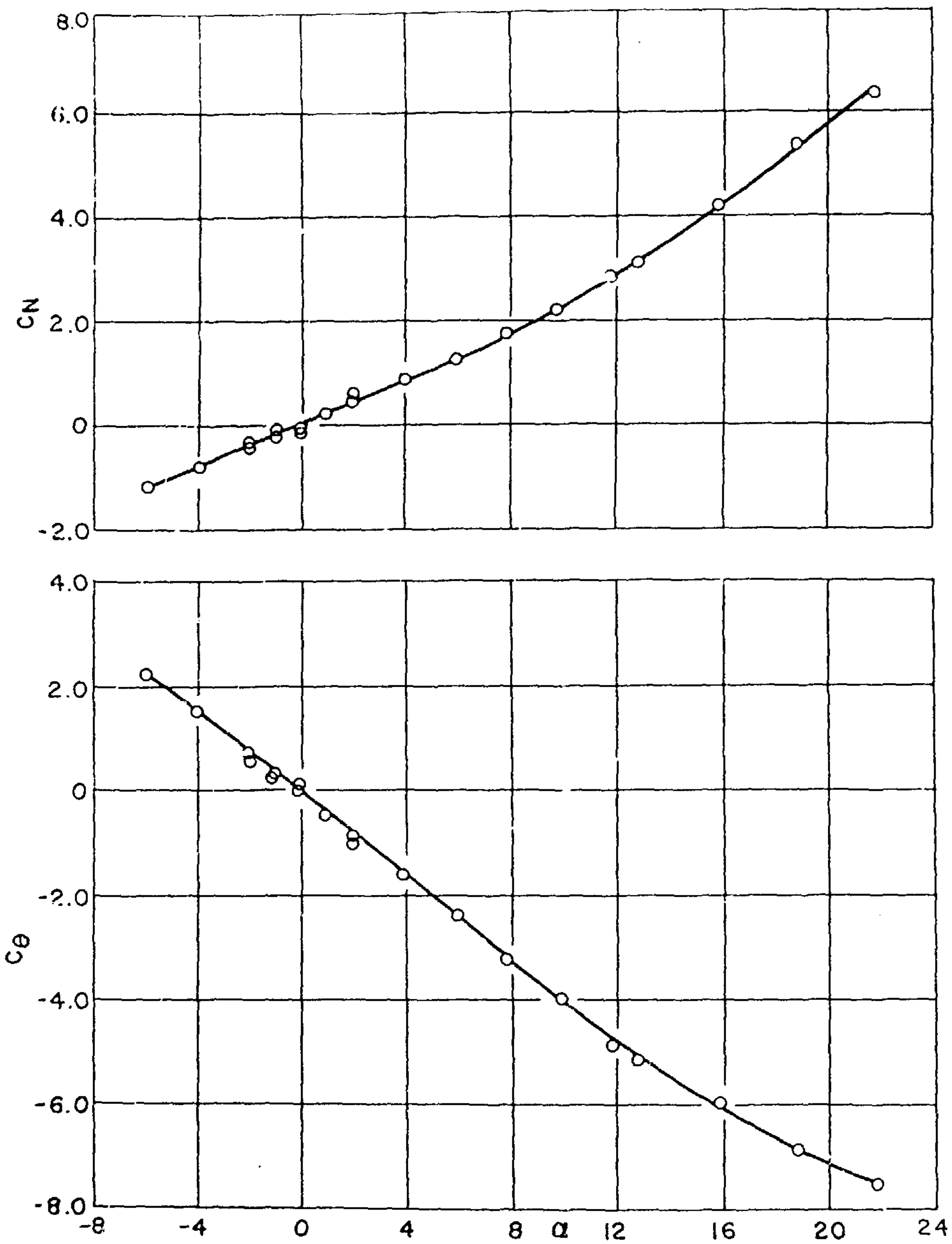

FIG. 5 BASIC FINNER
STATIC STABILITY
M = 1.76 Ø = 45°
C.G. = 6 CALIBERS FROM NOSE

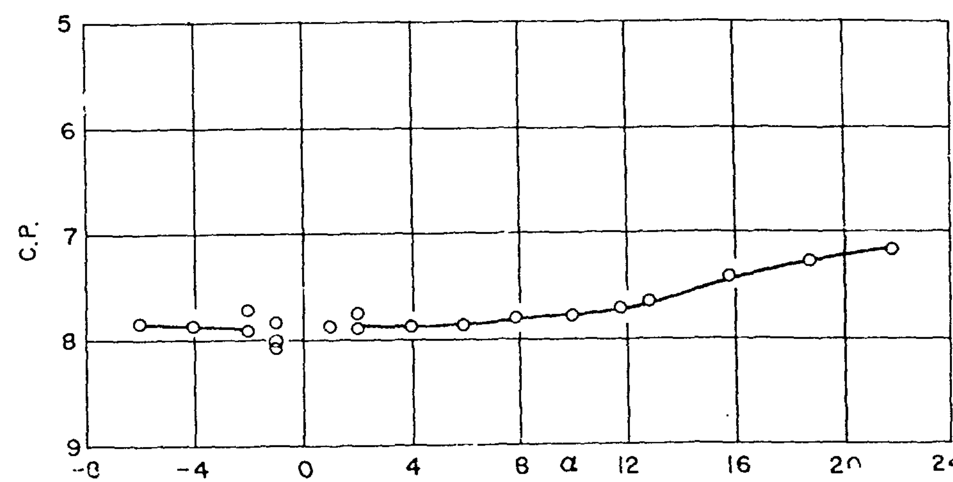

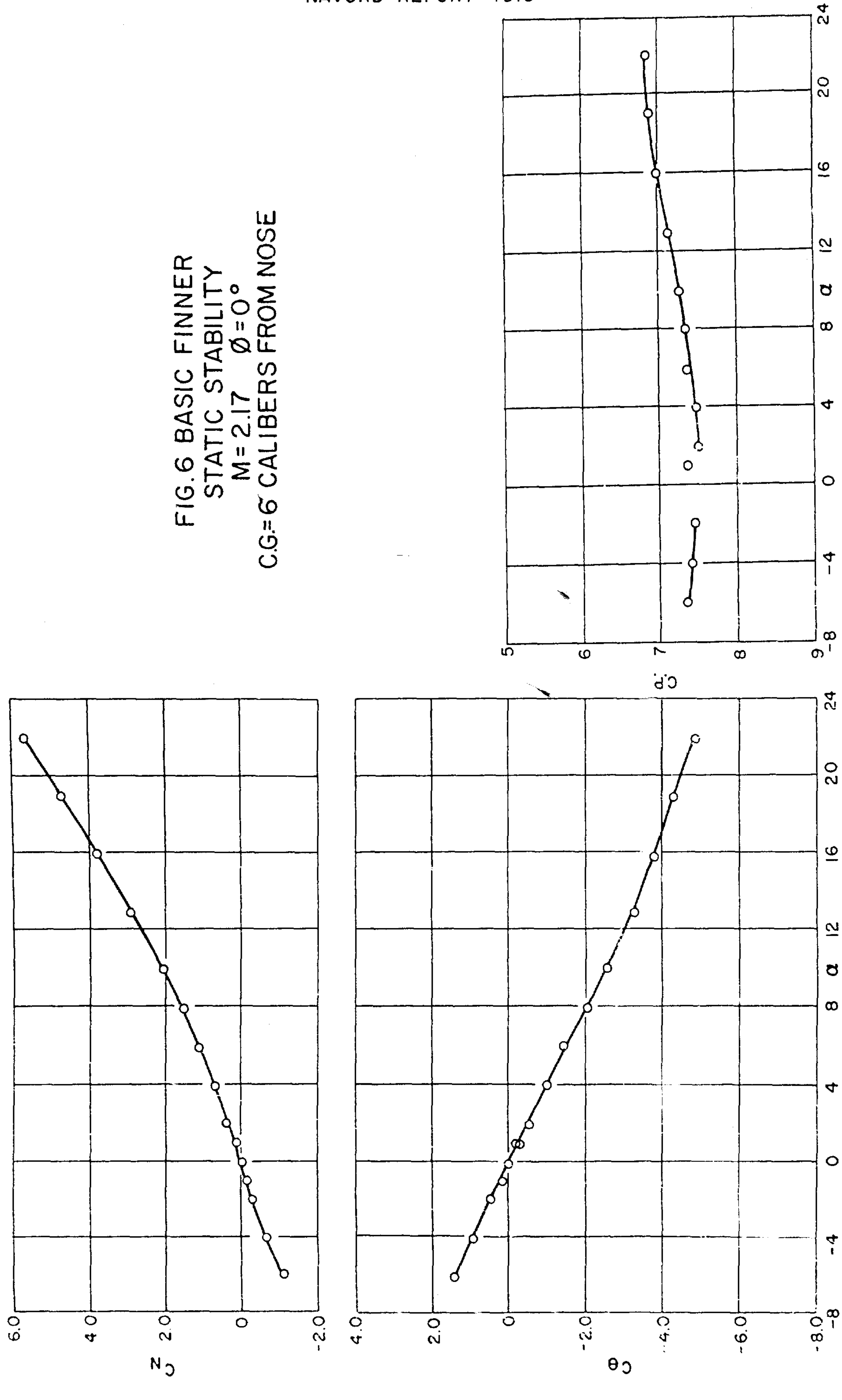

FIG. 6 BASIC FINNER
STATIC STABILITY
M = 2.17 Ø = 0°
C.G. = 6" CALIBERS FROM NOSE

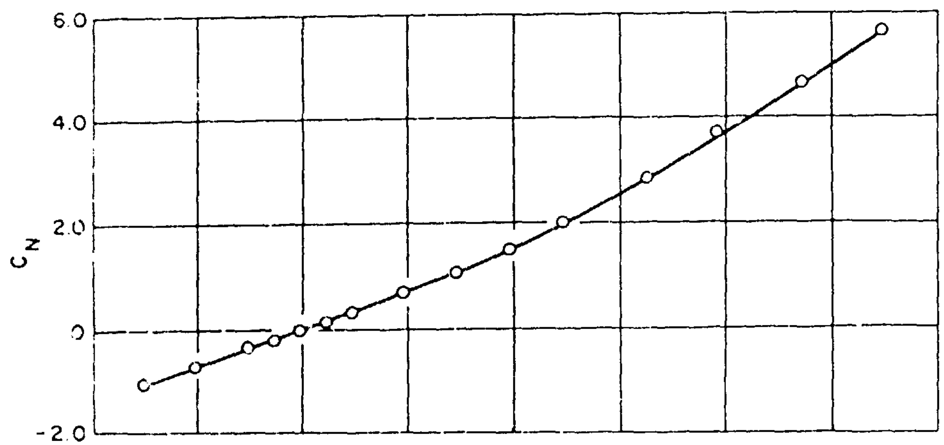

FIG. 7 BASIC FINNER
STATIC STABILITY
M = 2.17 Ø = 45°
C.G. = 6 CALIBERS FROM NOSE

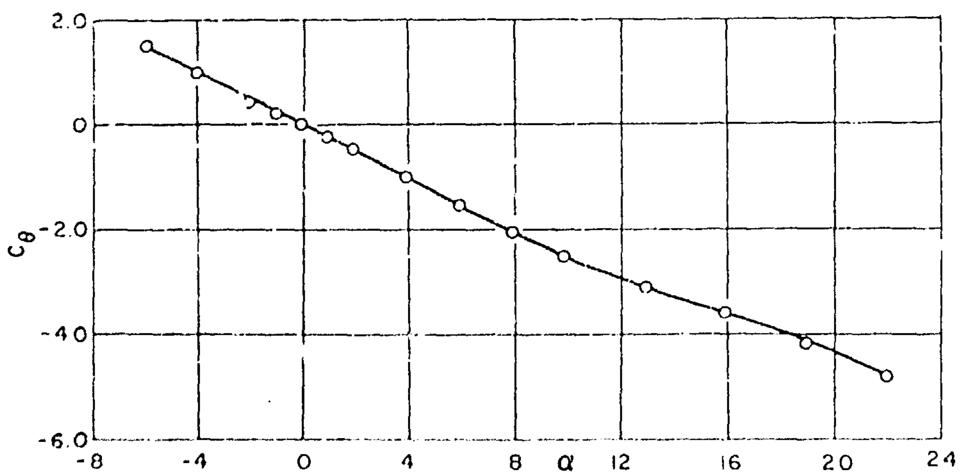

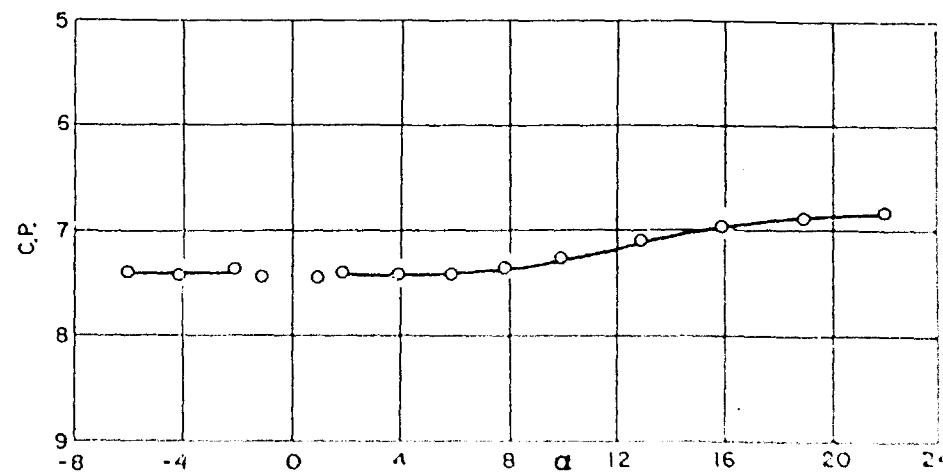

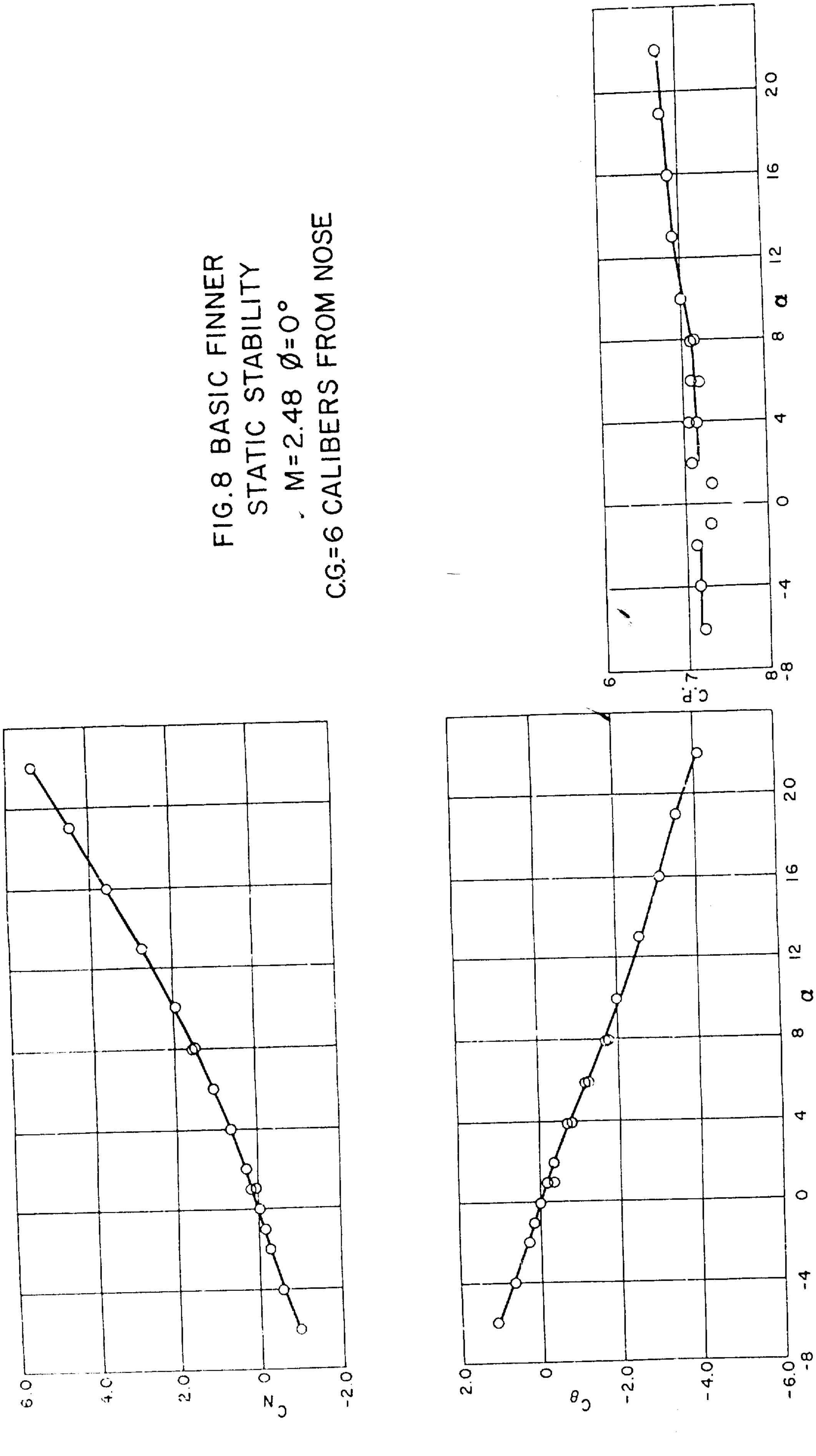

FIG.8 BASIC FINNER
STATIC STABILITY
M=2.48 Ø=0°
C.G.=6 CALIBERS FROM NOSE

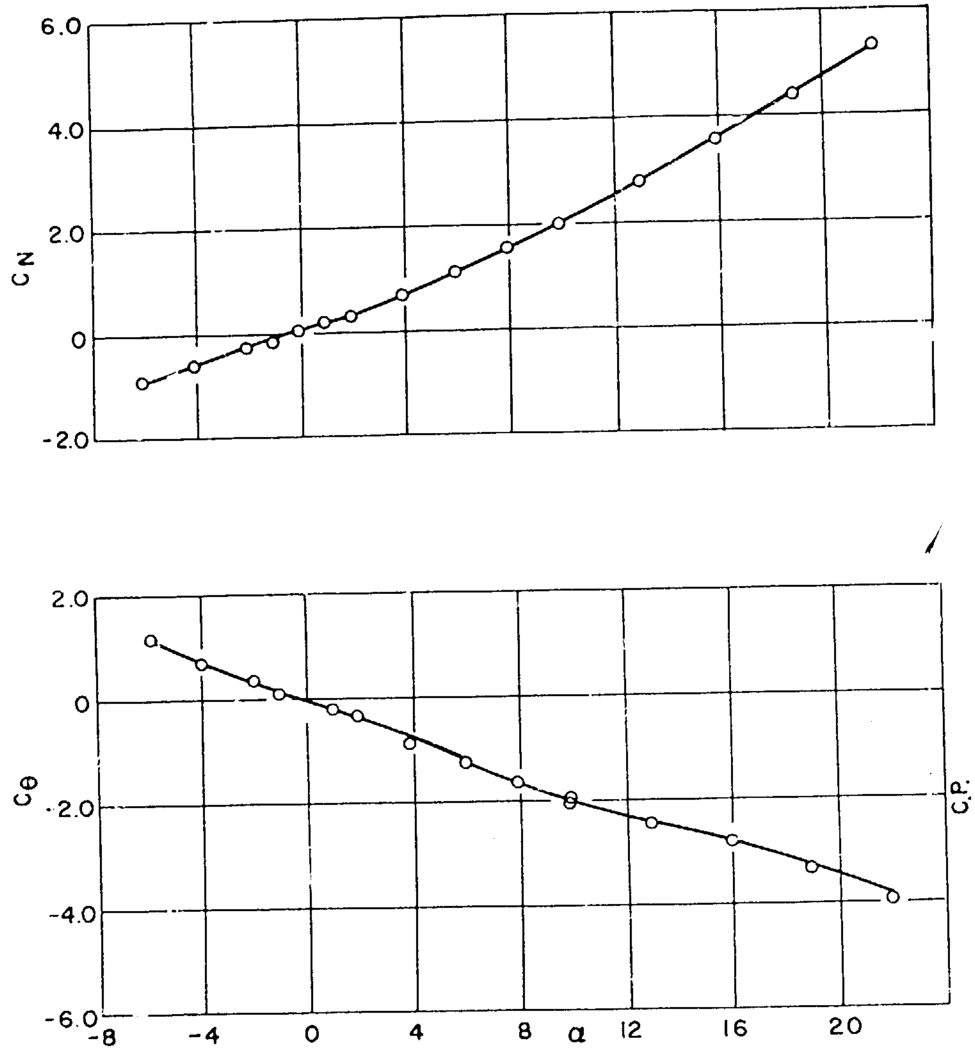

FIG. 9 BASIC FINNER
STATIC STABILITY
M=2.48 Ø=45°
C.G.=6 CALIBERS FROM NOSE

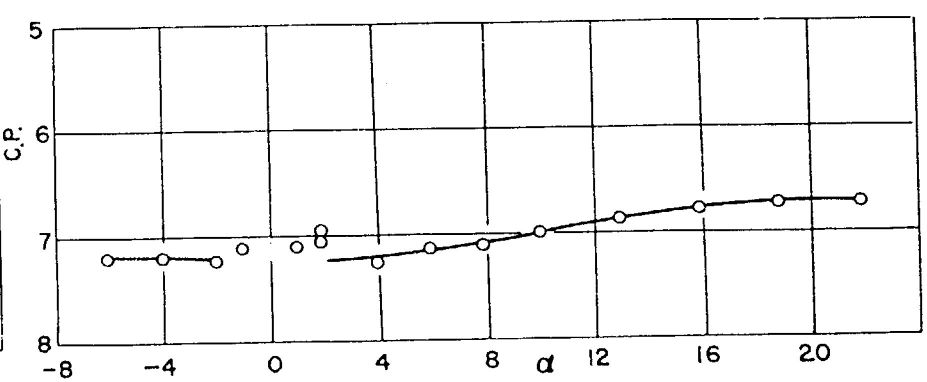

FIG. 10 BASIC FINNER
STATIC STABILITY
M=2.88 Ø=0°
C.G.=6 CALIBERS FROM NOSE

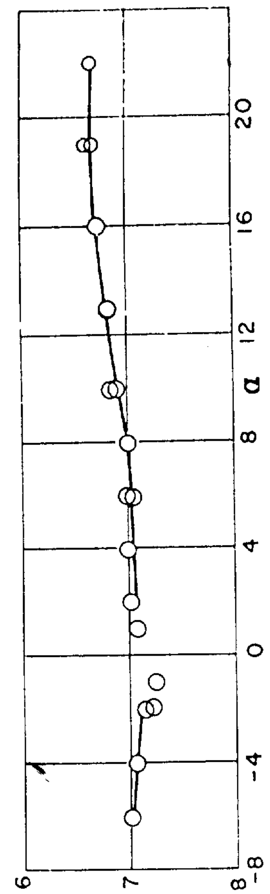

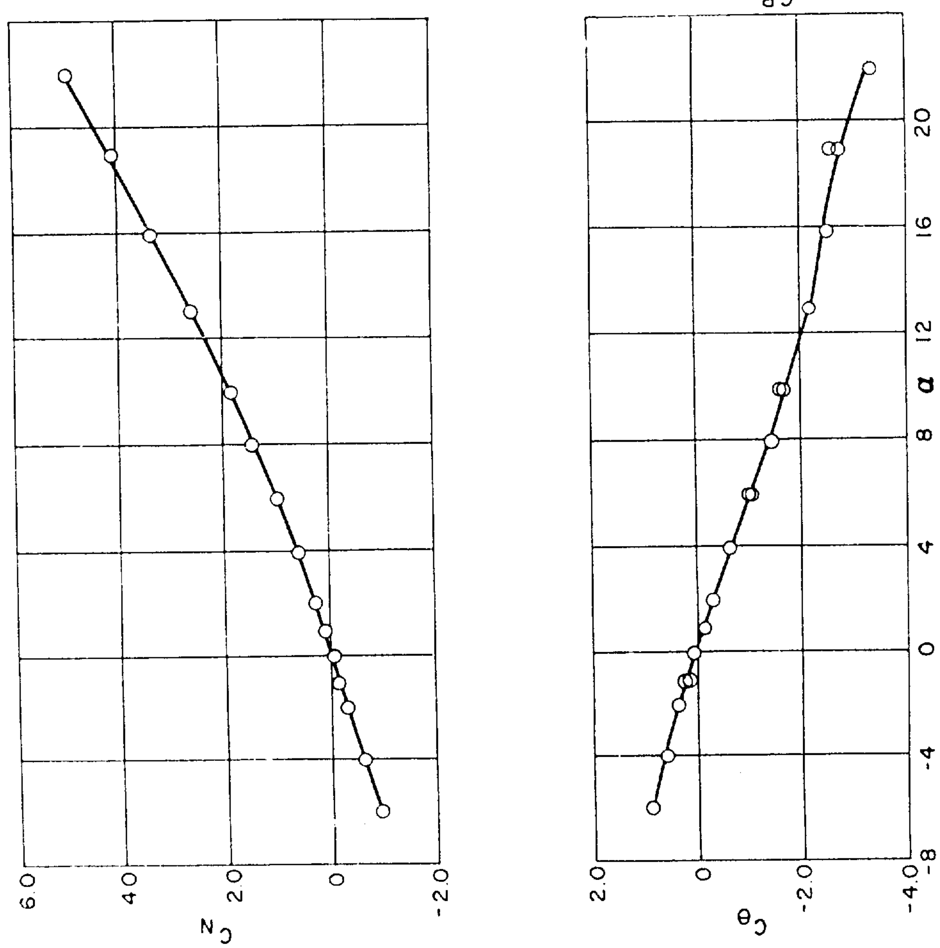

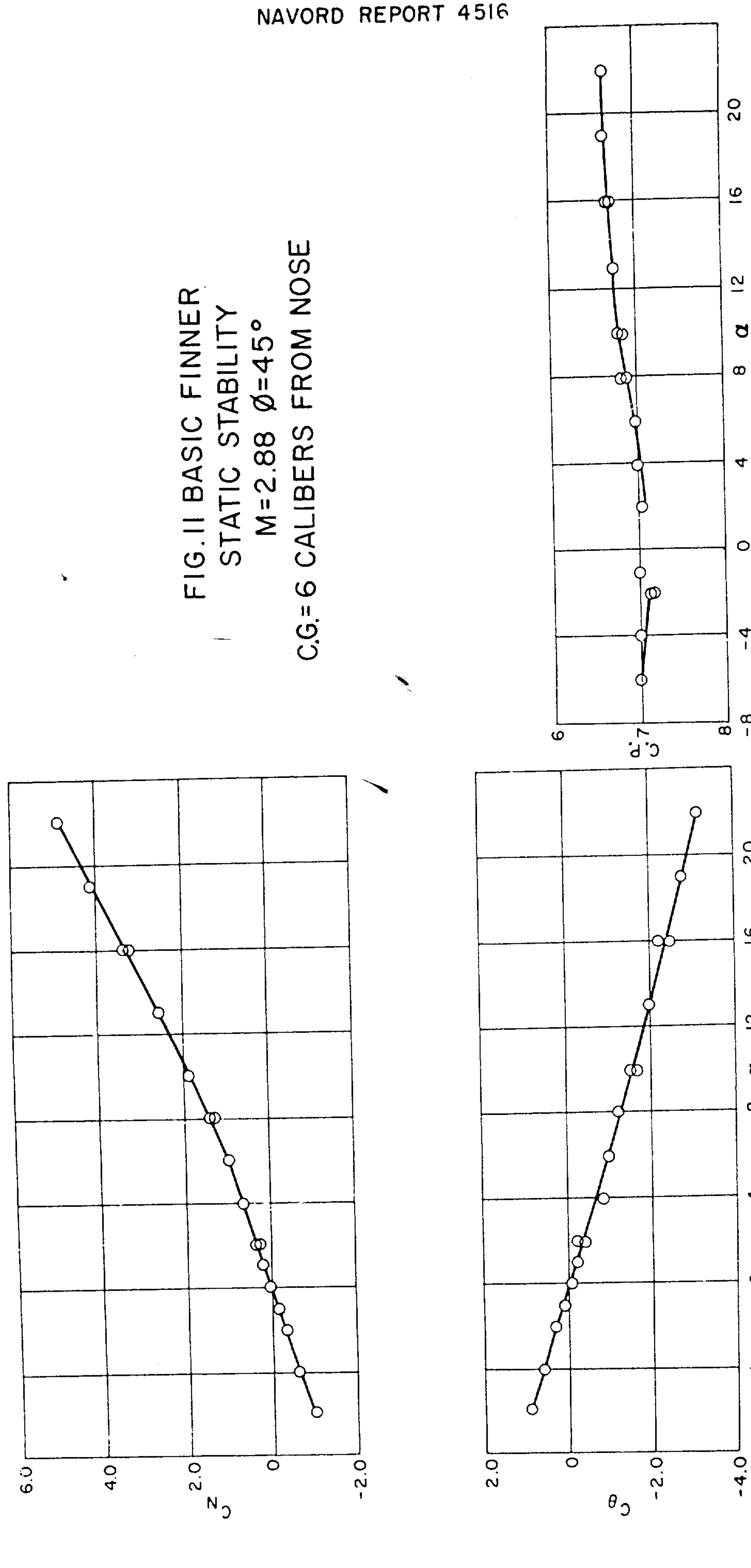

FIG. 11 BASIC FINNER
STATIC STABILITY
M=2.88 Ø=45°
C.G.=6 CALIBERS FROM NOSE

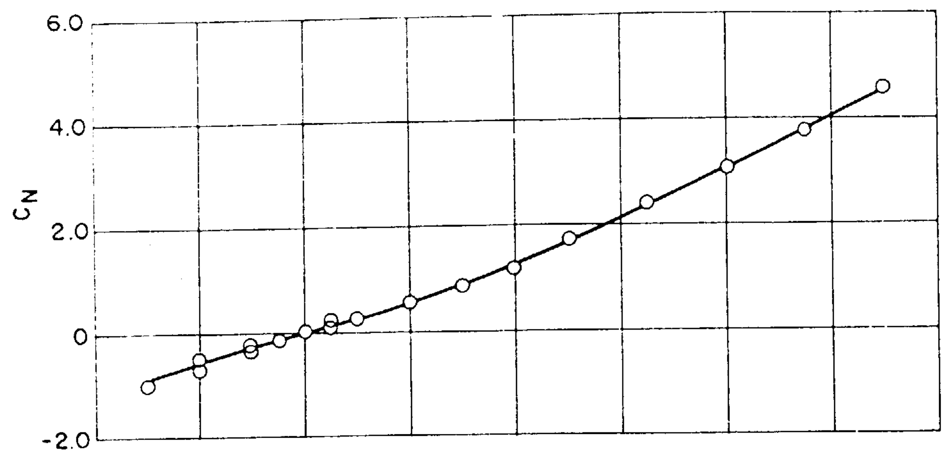

FIG. 12 BASIC FINNER
STATIC STABILITY
M = 3.22 Ø = 0°
C.G. = 6 CALIBERS FROM NOSE

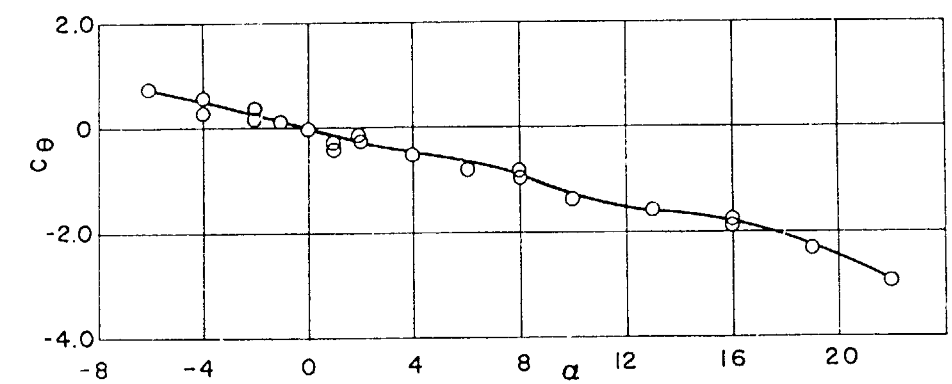

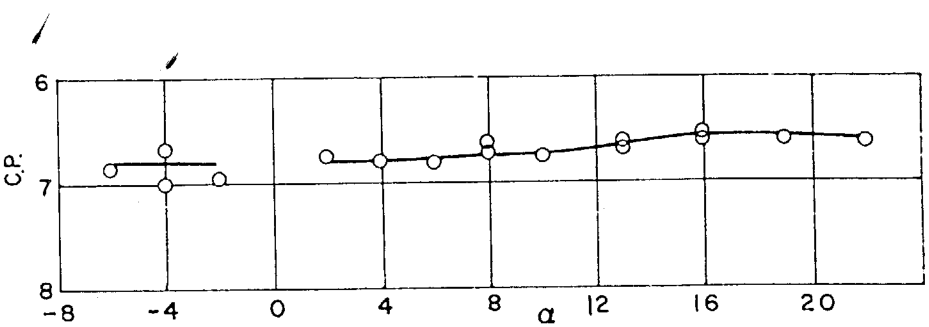

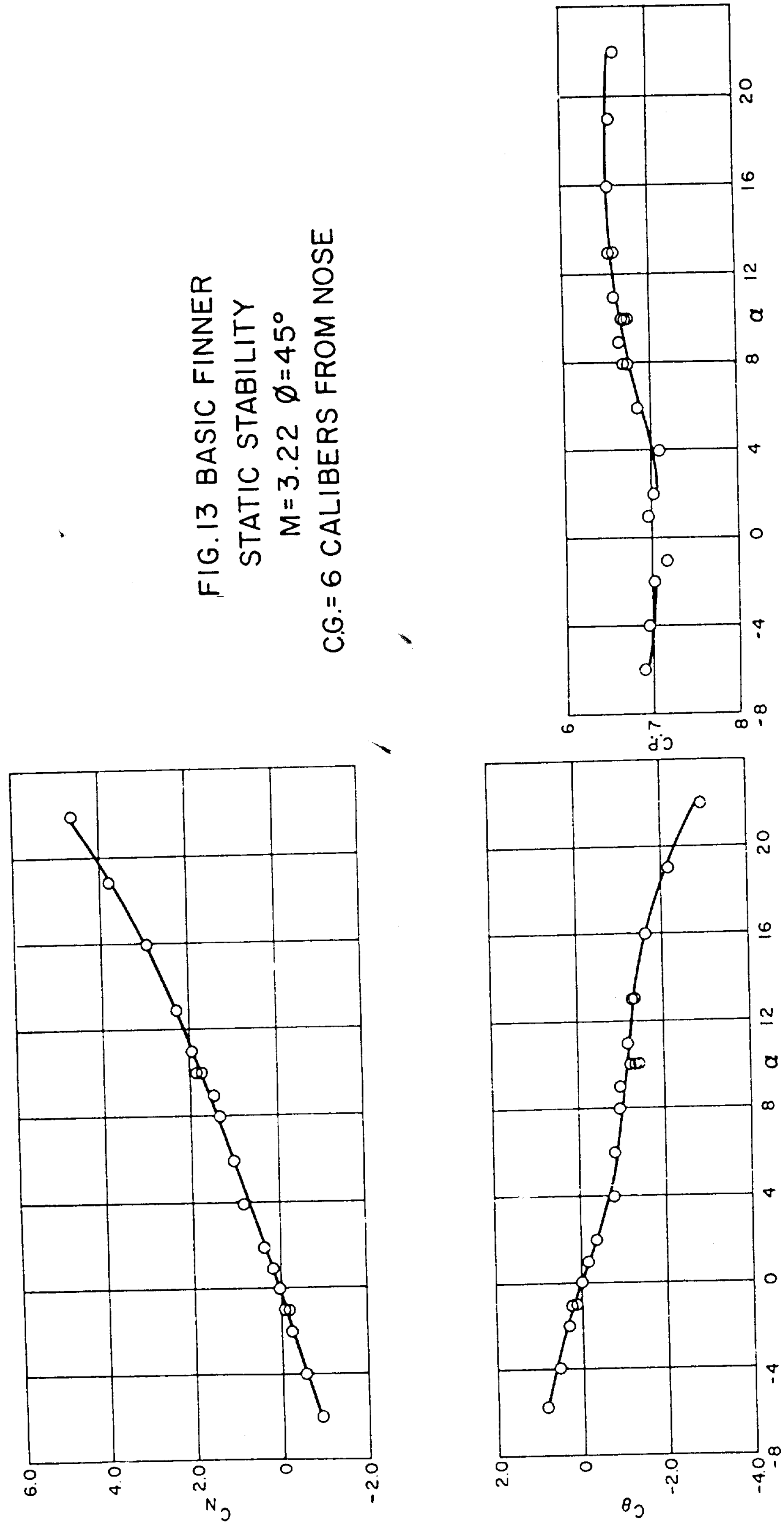

FIG. 13 BASIC FINNER
STATIC STABILITY
M = 3.22 Ø = 45°
C.G. = 6 CALIBERS FROM NOSE

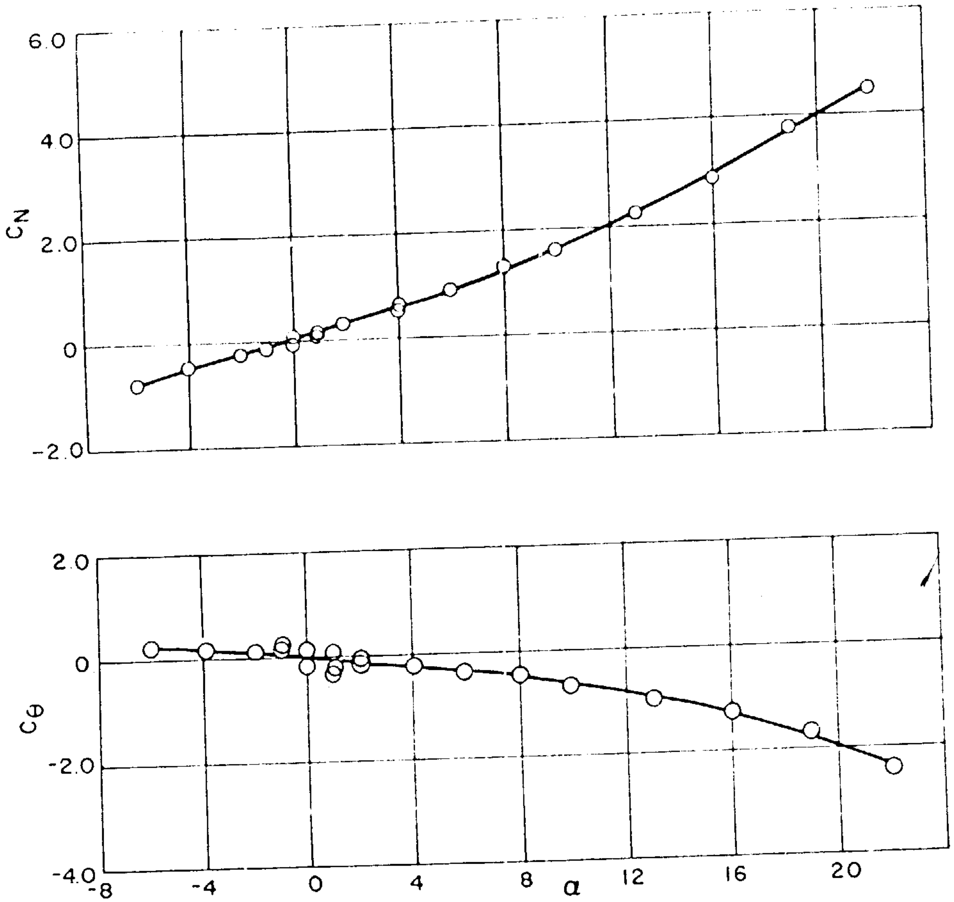

FIG.14 BASIC FINNER
STATIC STABILITY
M=3.86 ϕ=0°
C.G.= 6 CALIBERS FROM NOSE

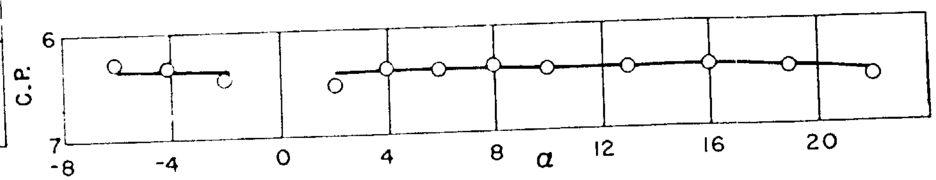

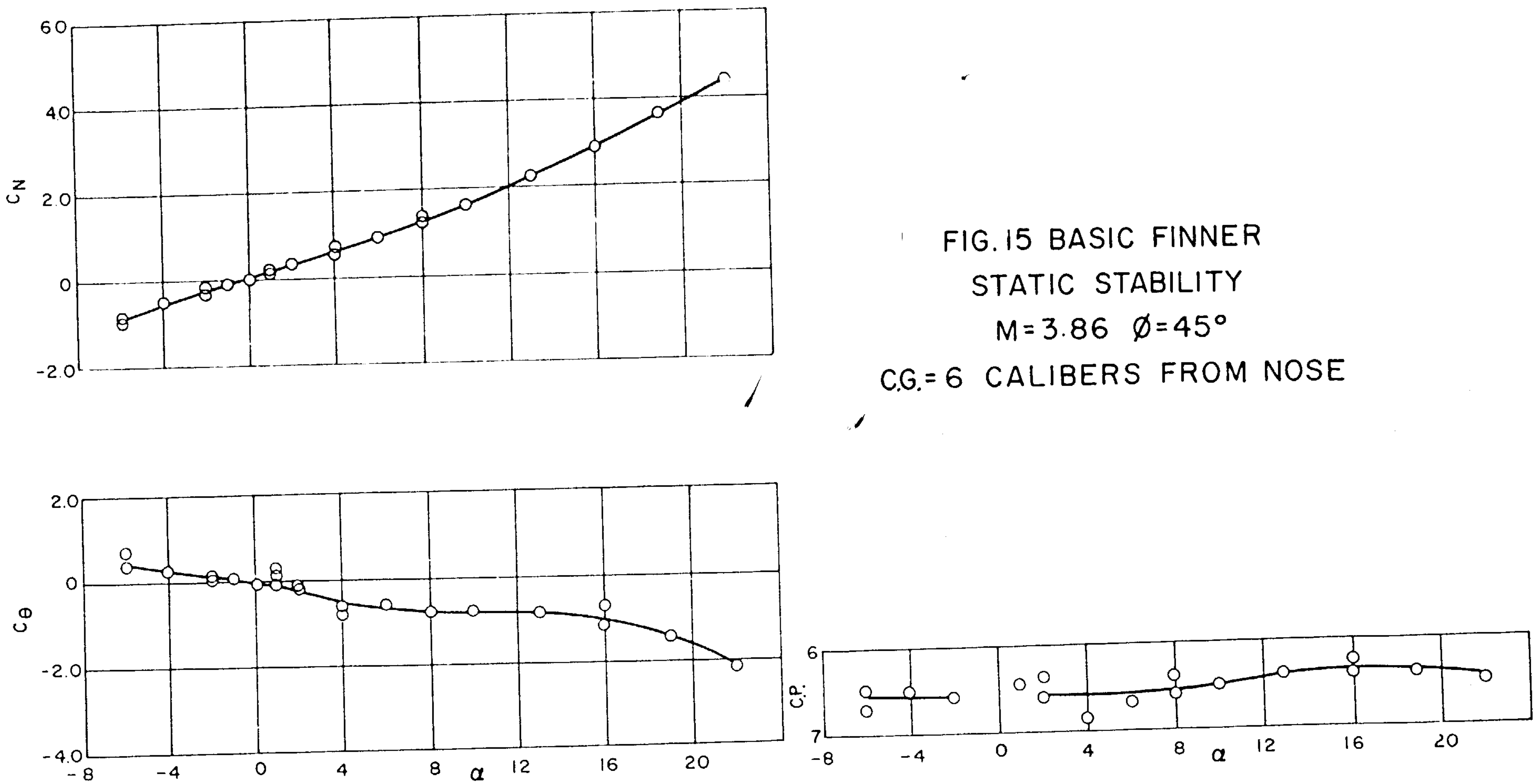

FIG. 15 BASIC FINNER
STATIC STABILITY
M = 3.86 Ø = 45°
C.G. = 6 CALIBERS FROM NOSE

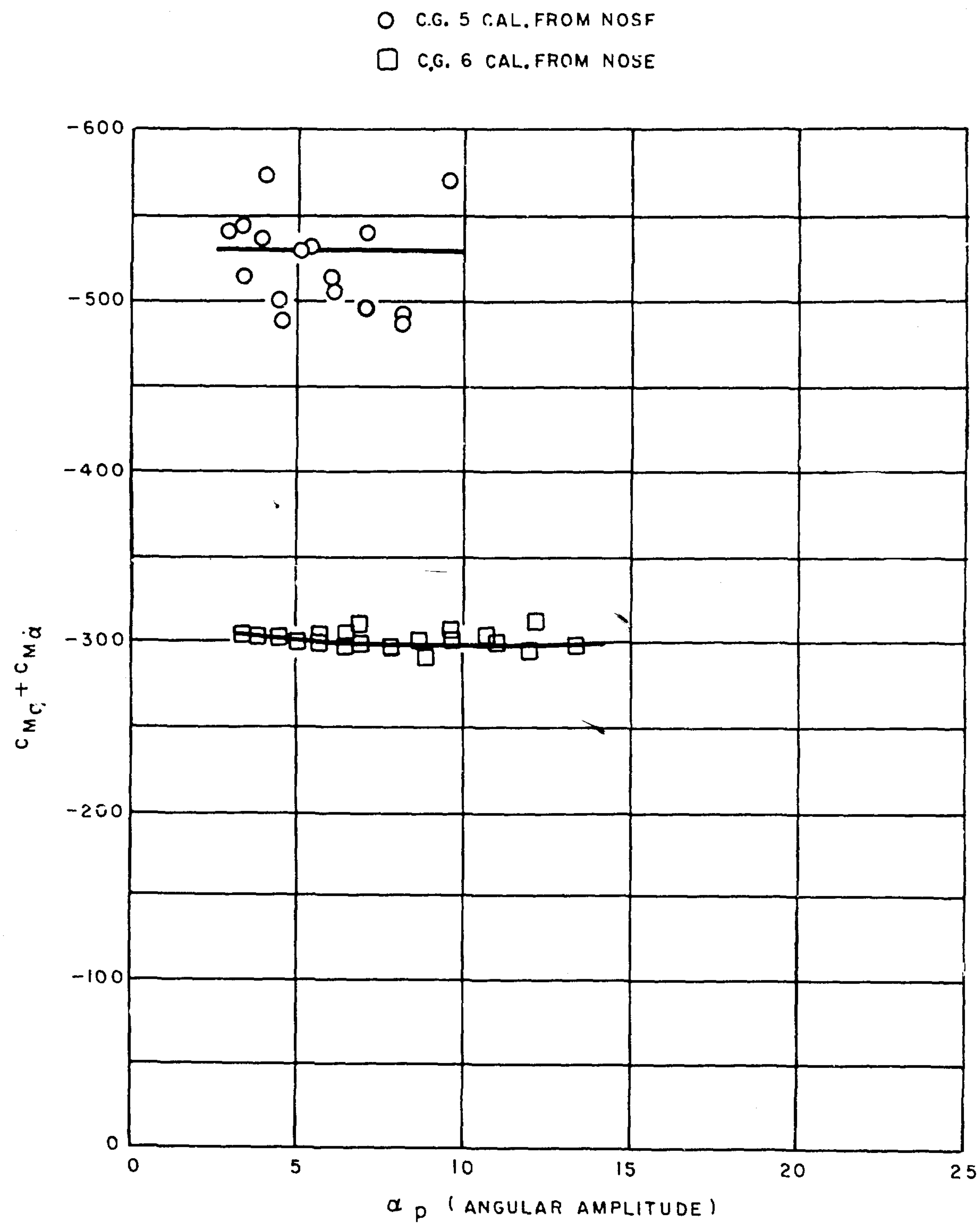

FIG. 16 BASIC FINNER
$C_{M_q} + C_{M_{\dot{\alpha}}}$ VS ANGULAR AMPLITUDE
MACH NO.= 1.58

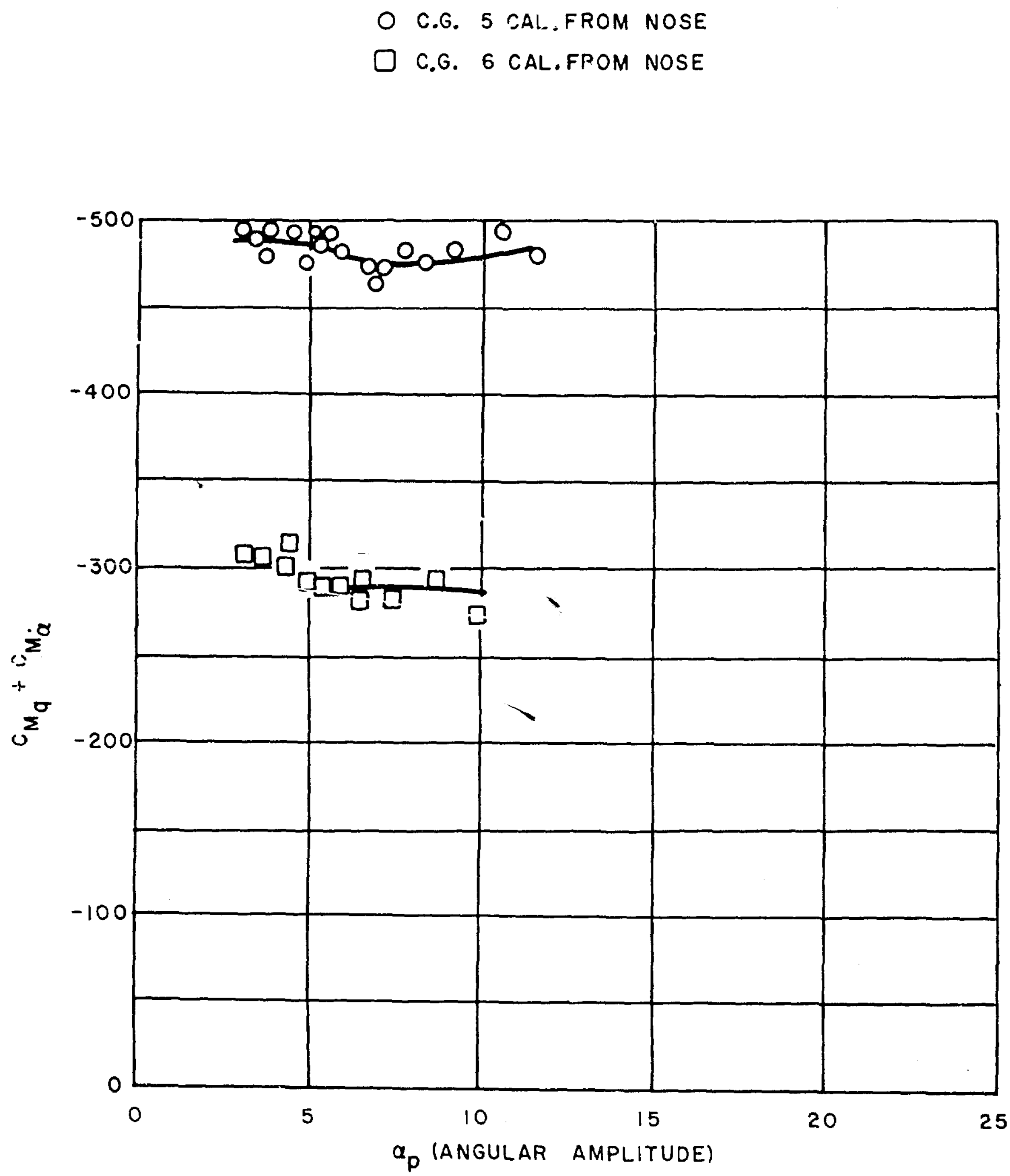

FIG. 17 BASIC FINNER

$C_{M_q} + C_{M_{\dot{\alpha}}}$ VS ANGULAR AMPLITUDE

MACH NO.=1.76

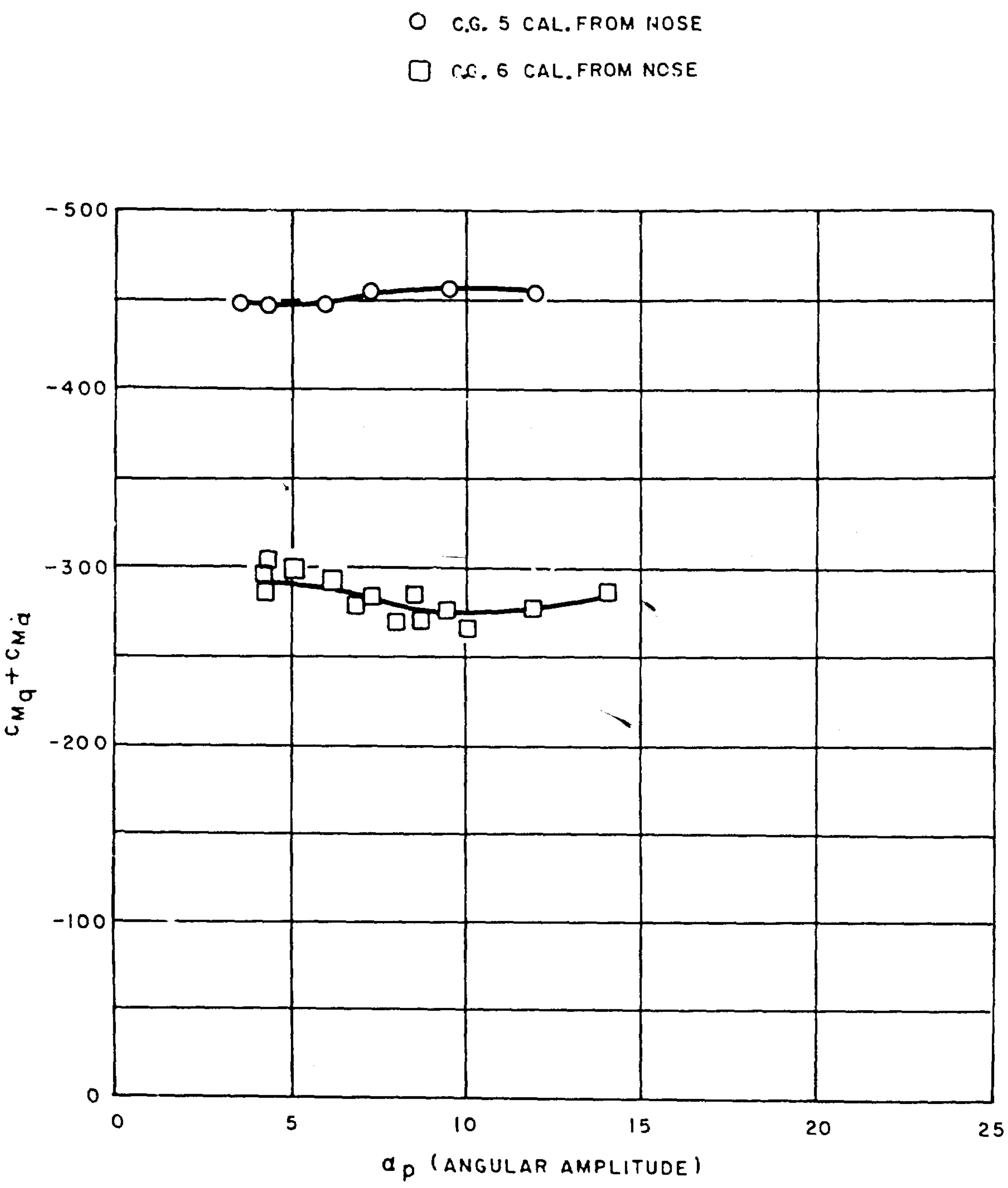

FIG. 18 BASIC FINNER
$C_{M_q} + C_{M_{\dot{\alpha}}}$ VS ANGULAR AMPLITUDE
MACH NO.= 1.89

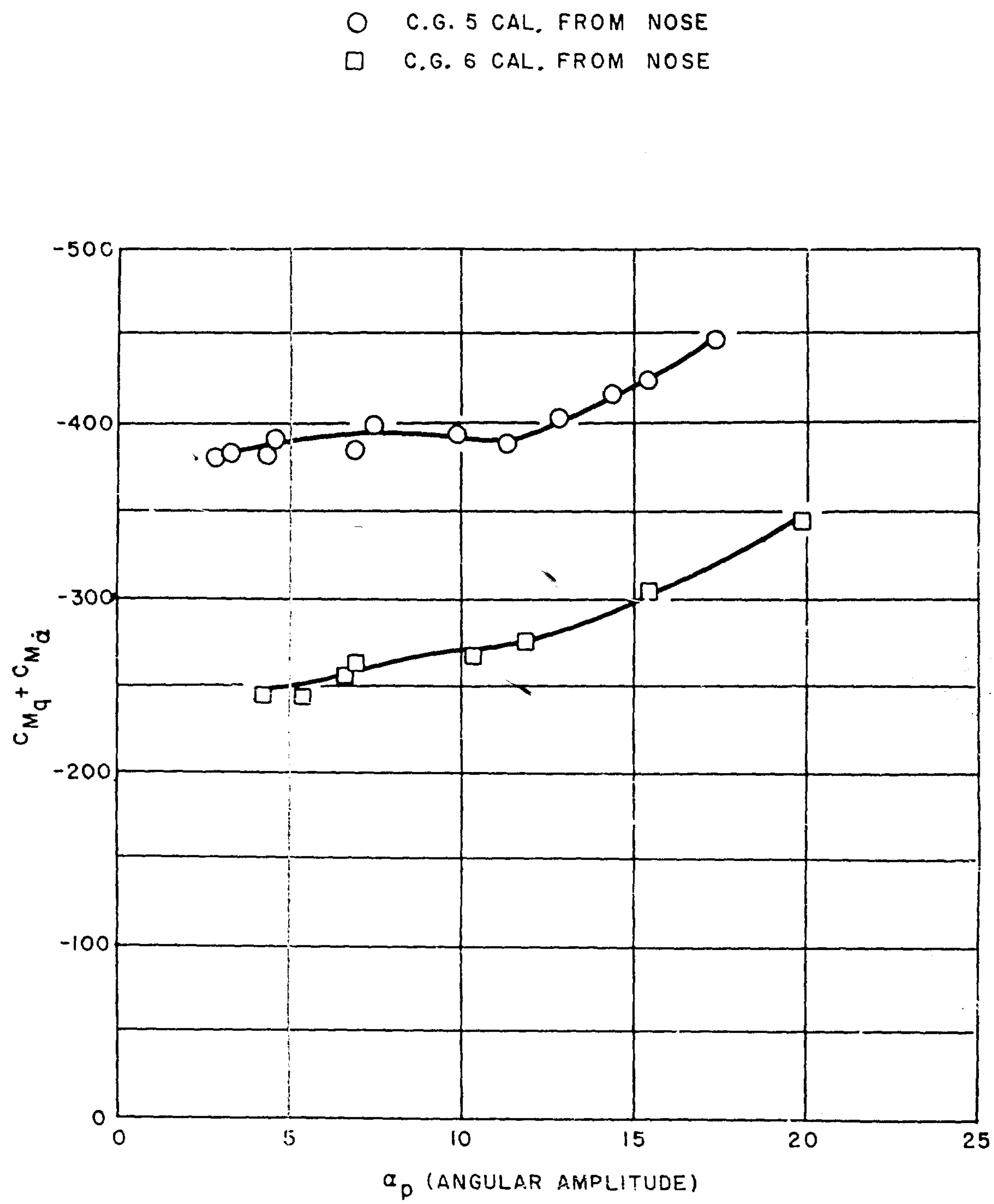

FIG. 19 BASIC FINNER

$C_{M_q} + C_{M_{\dot{\alpha}}}$ VS ANGULAR AMPLITUDE

MACH NO.=2.16

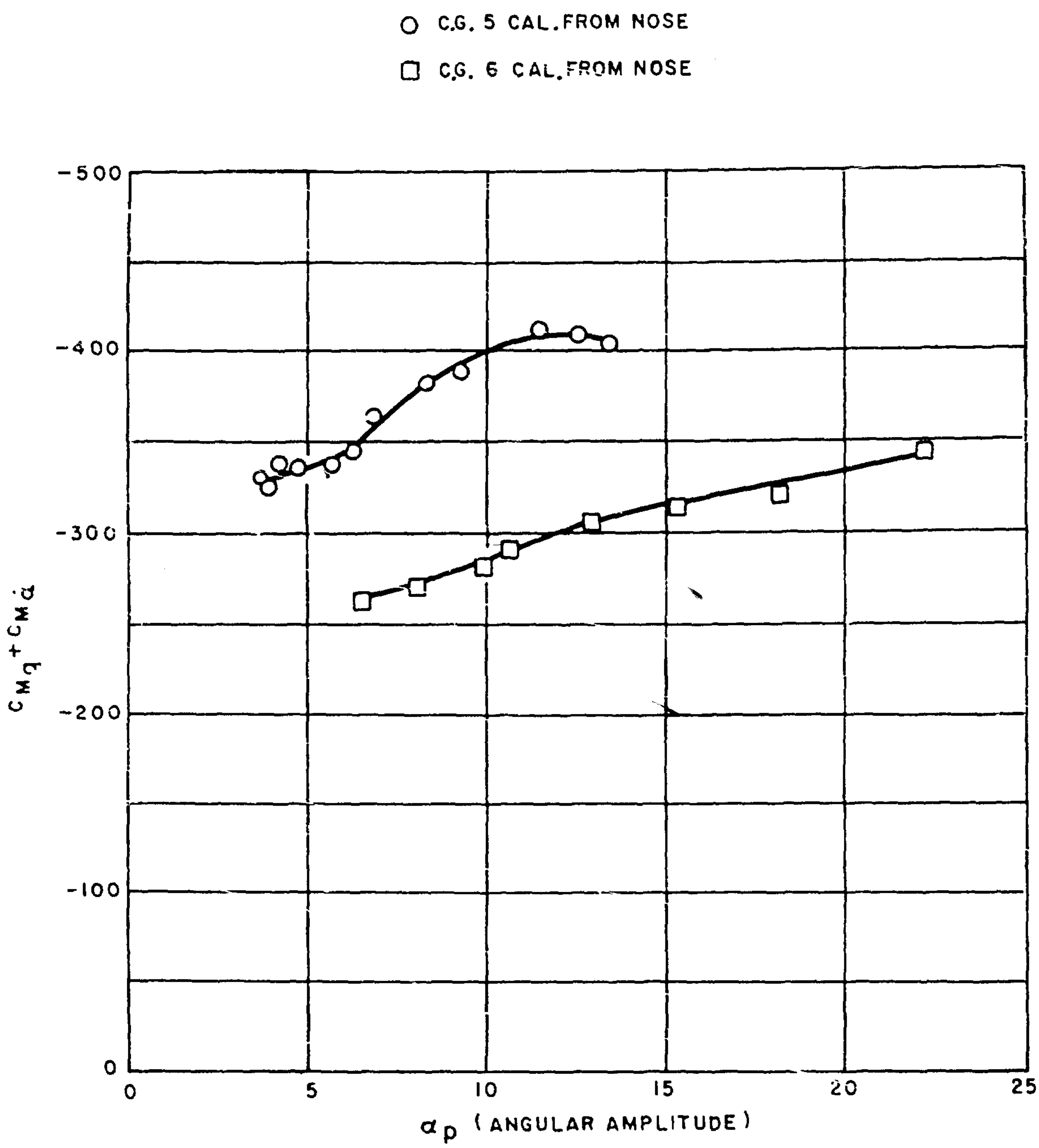

FIG. 20 BASIC FINNER

$C_{M_q} + C_{M_{\dot{\alpha}}}$ VS ANGULAR AMPLITUDE

MACH NO. = 2.48

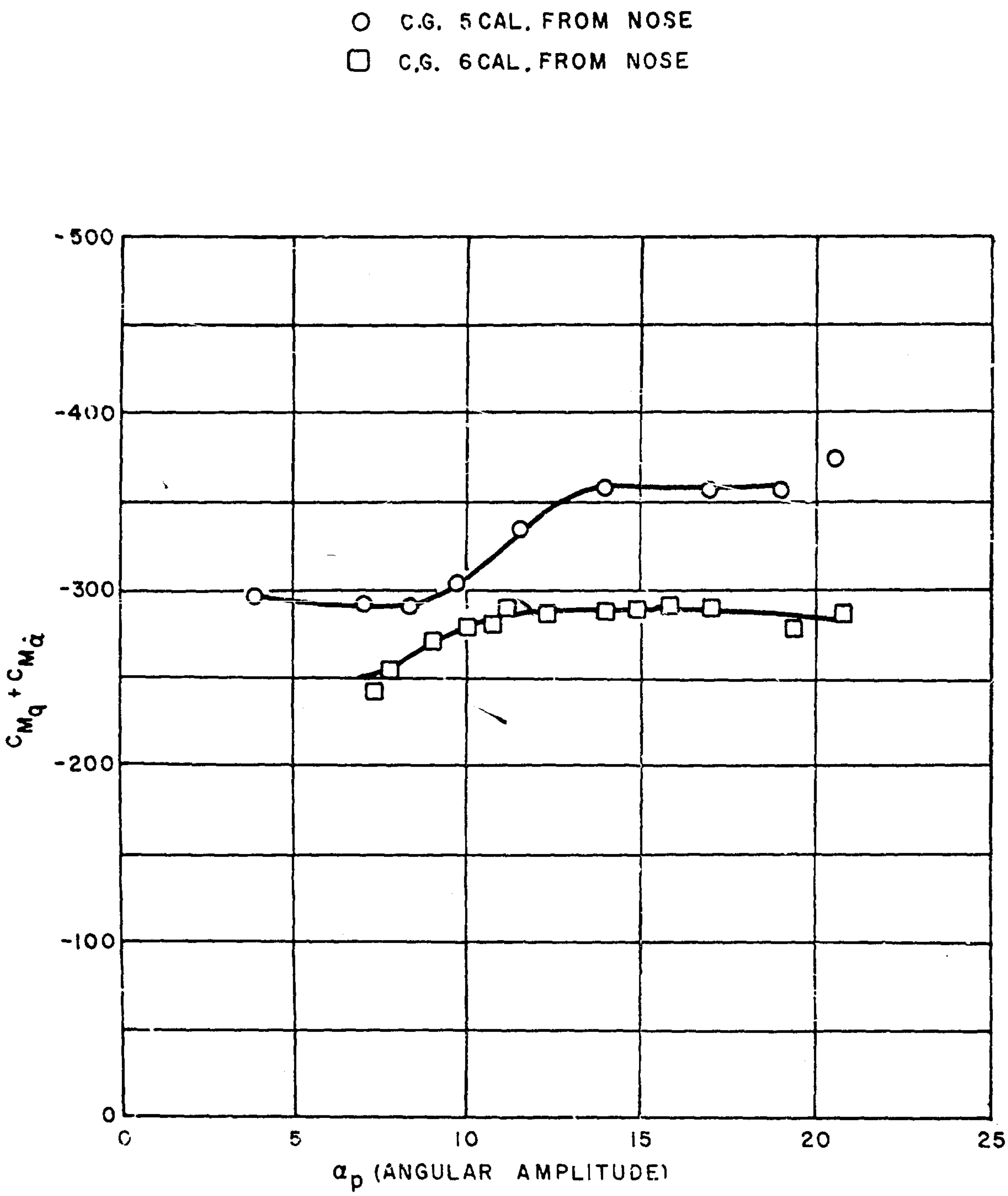

FIG. 21 BASIC FINNER

$C_{M_q} + C_{M_{\dot{\alpha}}}$ VS ANGULAR AMPLITUDE

MACH NO.=2.88

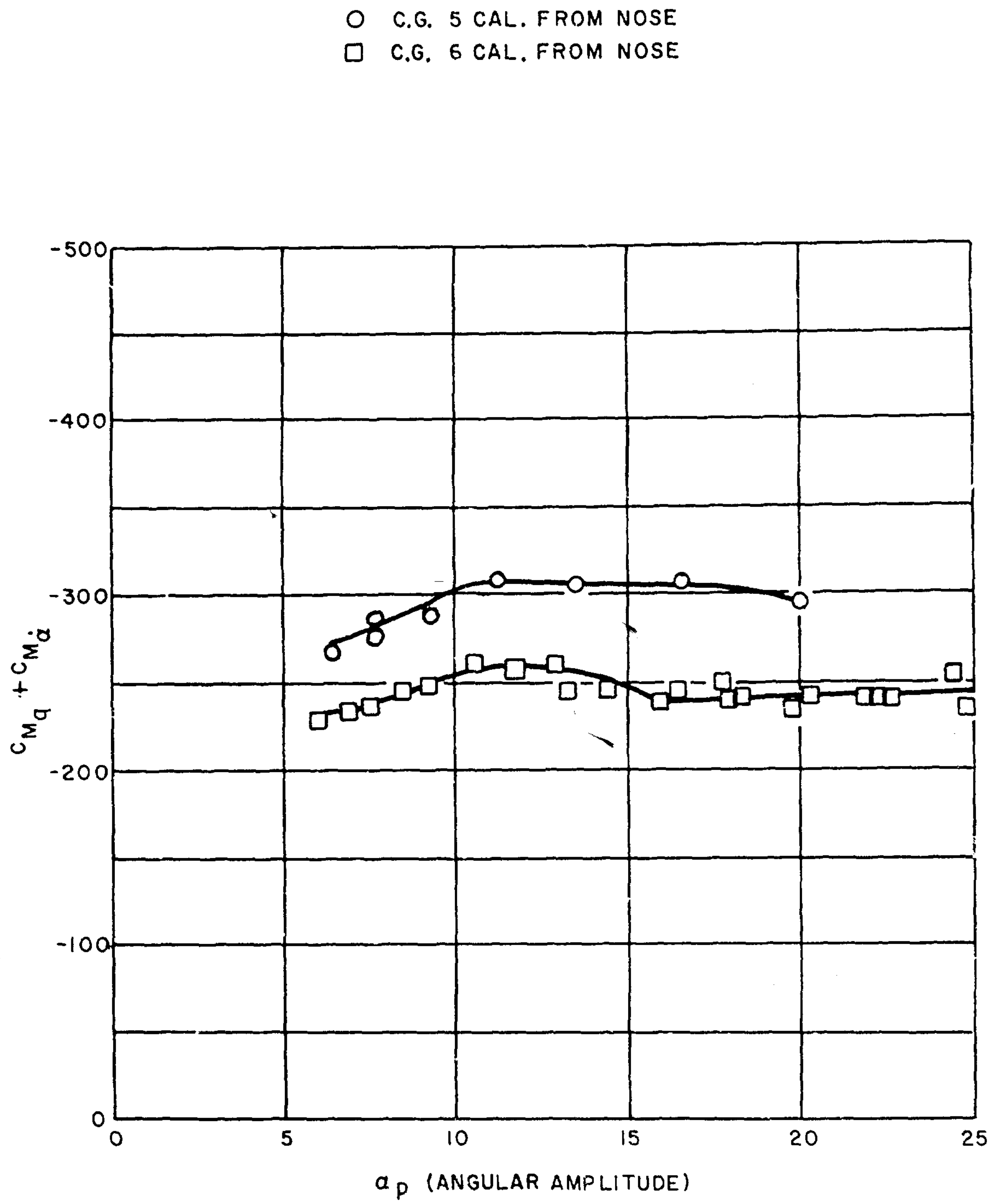

FIG. 22 BASIC FINNER

$C_{M_q} + C_{M_{\dot{\alpha}}}$ VS ANGULAR AMPLITUDE

MACH NO.= 3.24

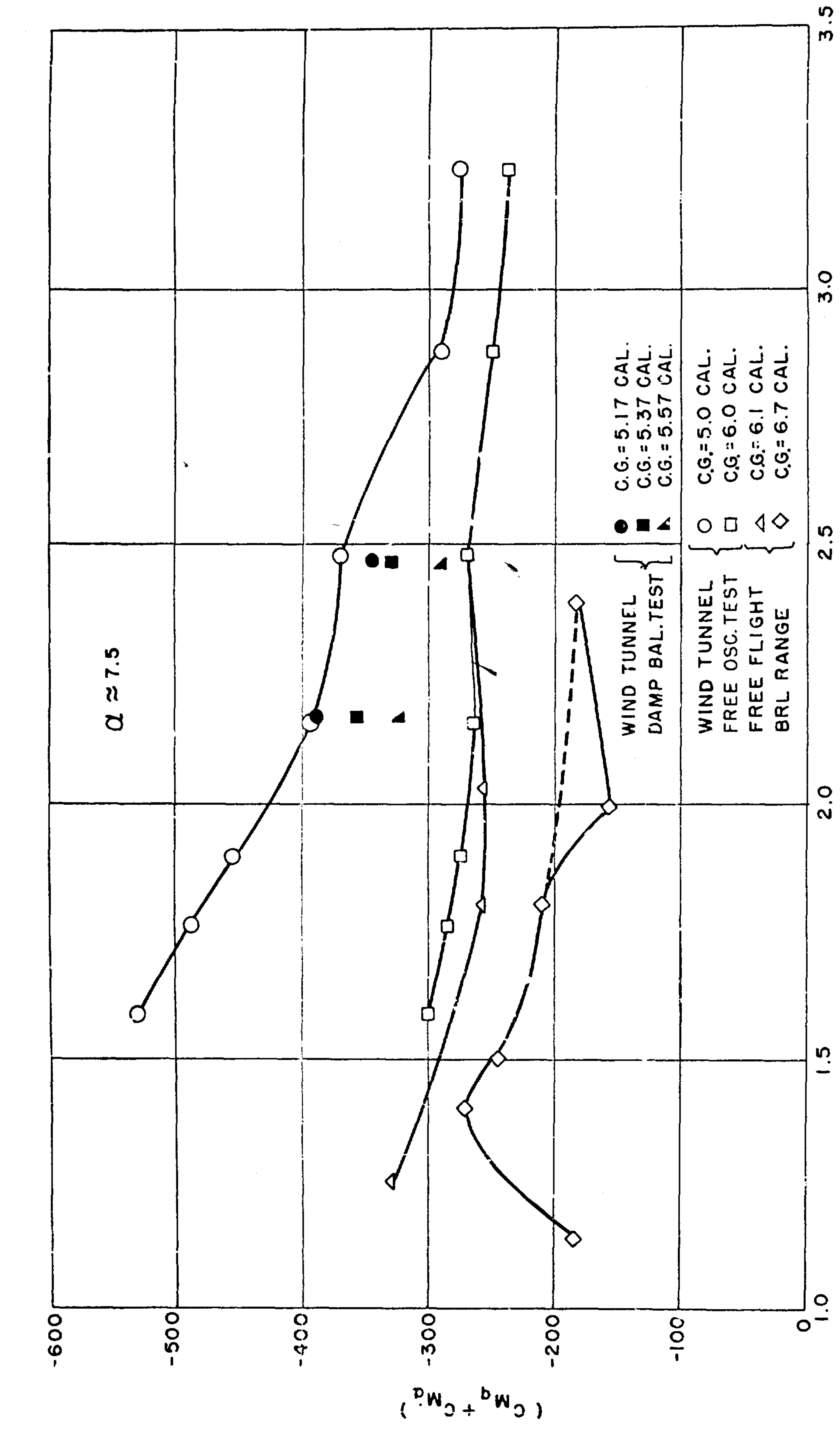

FIG. 23 $C_{M_q} + C_{M_{\dot\alpha}}$ VS MACH NUMBER

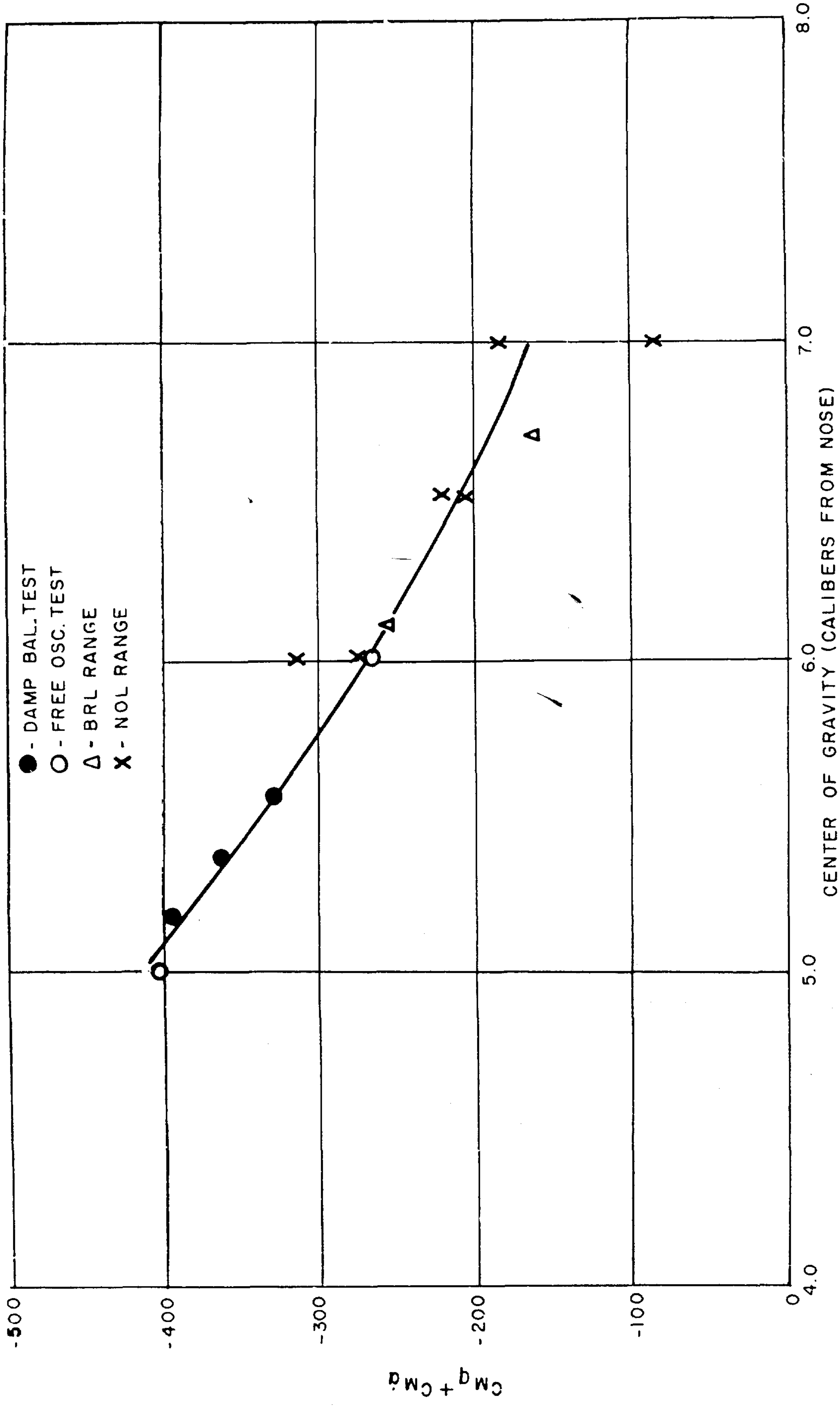

FIG. 24 $C_{M_q}+C_{M_{\dot\alpha}}$ VS CENTER OF GRAVITY

$M \simeq 2.1$

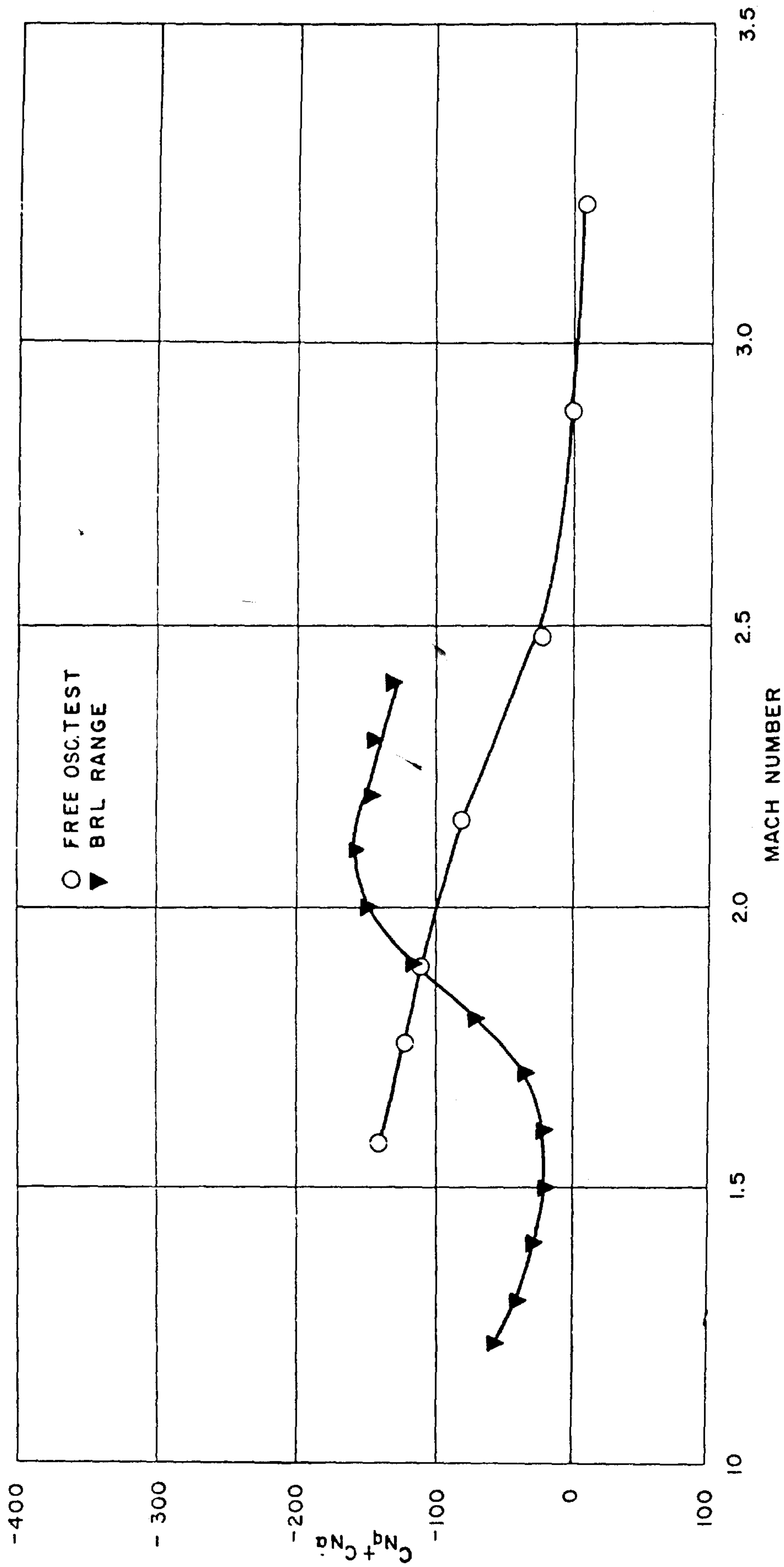

FIG. 25 $C_{N_q} + C_{N_{\dot\alpha}}$ VS MACH NUMBER

AT CENTROID OF PROJECTED AREA, 6.39 CAL. FROM NOSE

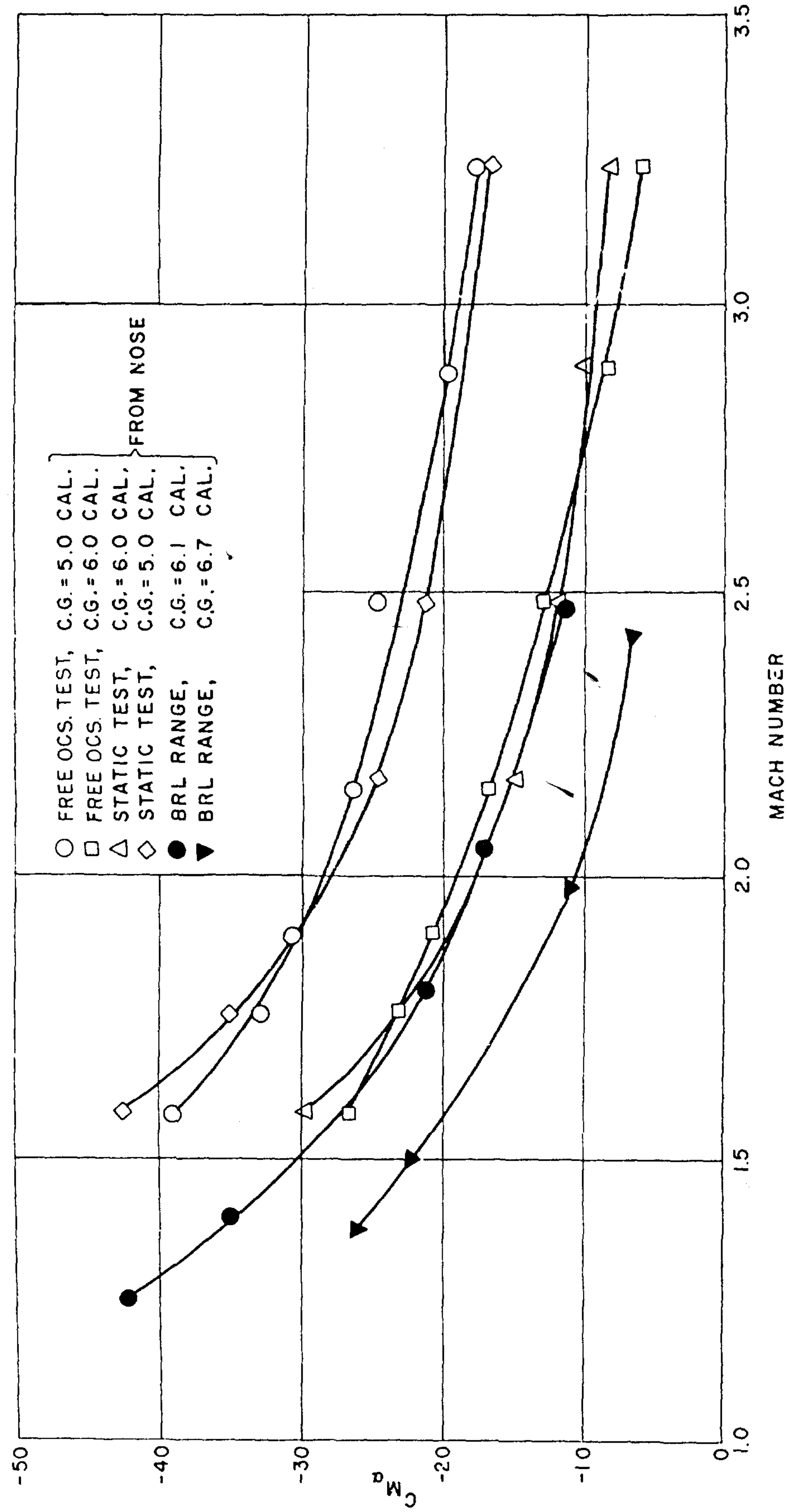

FIG. 26 C_{M_α} VS MACH NUMBER

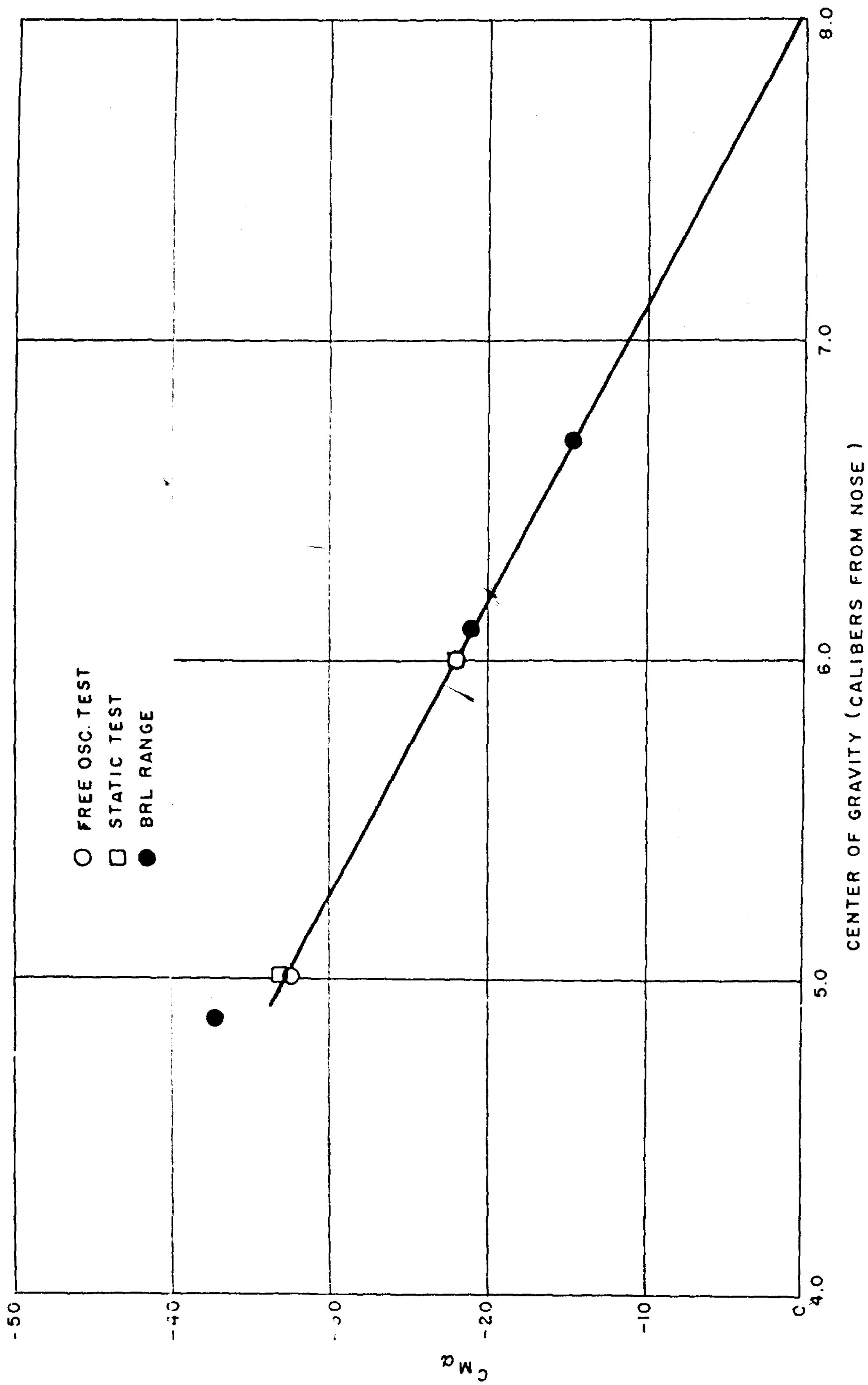

FIG.27 C_{M_α} VS CENTER OF GRAVITY, M=1.8

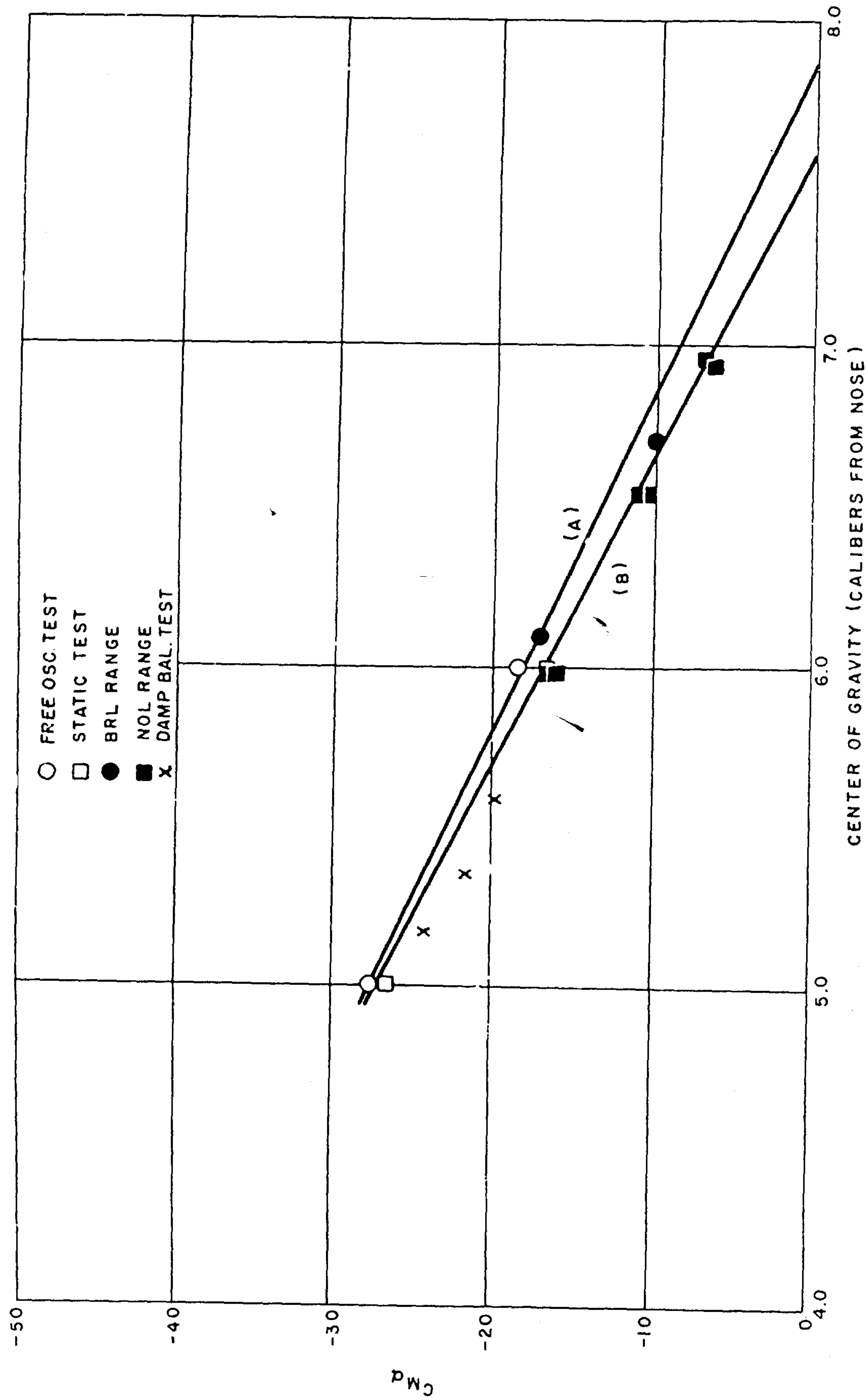

FIG. 28 C_{M_α} VS CENTER OF GRAVITY, $M \simeq 2.1$

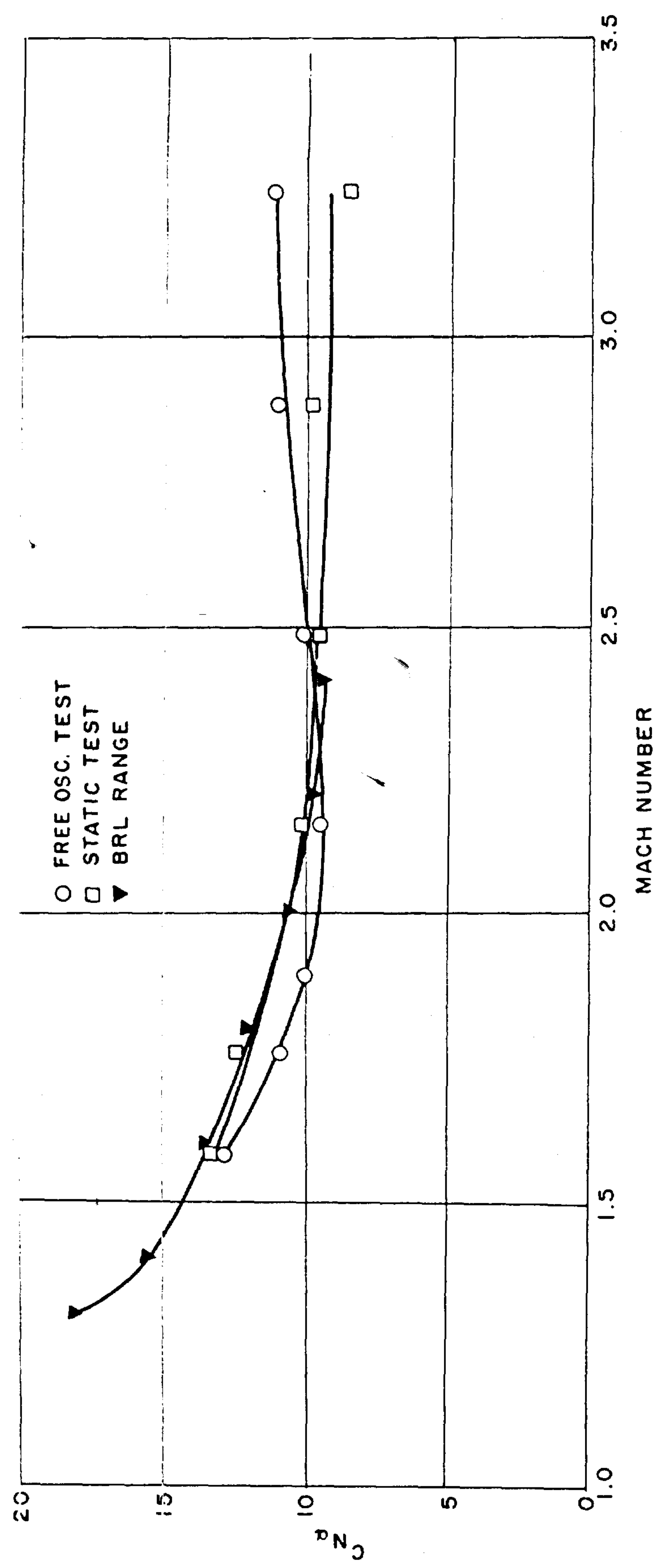

FIG.29 C_{N_α} VS MACH NUMBER

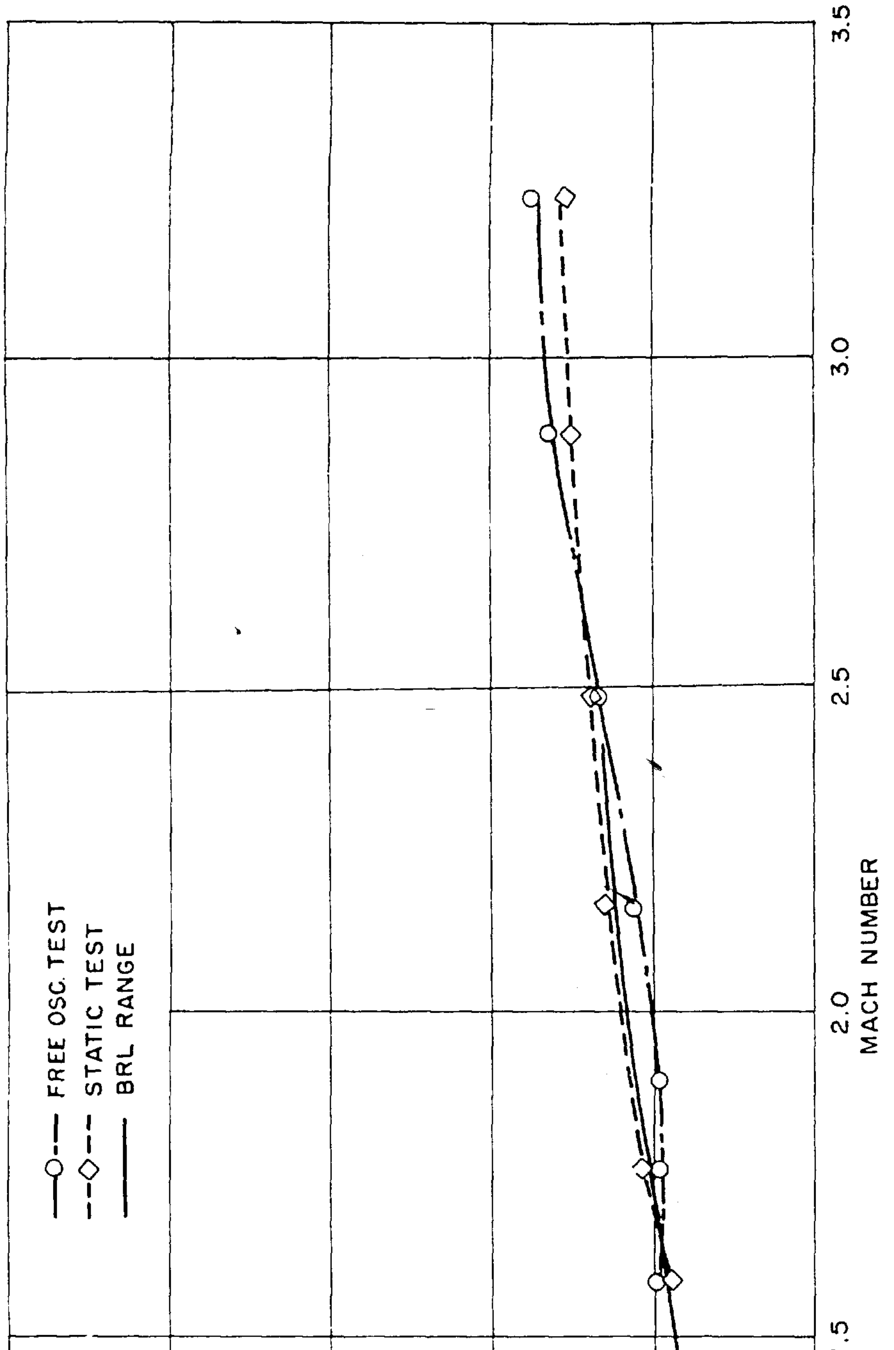

FIG. 30 CENTER OF PRESSURE VS MACH NUMBER

External Distribution List

No. of Copies	
	Chief, Bureau of Naval Weapons Department of the Navy Washington 25, D. C.
1	Attn: RT-1
2	Attn: RMMO-42
3	Attn: RRRE-7
1	Attn: RMMS-53
1	Attn: DL1-30
1	Attn: R-14
1	Attn: Document Library
	Office of Naval Research Room 2709, T-3 Washington 25, D. C. Attn: Head, Mechanics Br.
	Director, DTMB Aerodynamics Laboratory Washington 7, D. C.
1	Attn: Library
	Naval Weapons Laboratory Dahlgren, Virginia
1	Attn: Library
	Commander, U. S. NOTS China Lake, California
1	Attn: Technical Library
1	Attn: Code 503
1	Attn: Code 406
	Director, NRL Washington 25, D. C.
1	Attn: Code 2027
12	Commanding Officer Office of Naval Research Branch Office Box 39, Navy 100 Fleet Post Office New York, N. Y.
	NASA High Speed Flight Station Box 273 Edwards Air Force Base, California
1	Attn: W. C. Williams
	NASA Ames Aeronautical Laboratory Moffett Field, California
1	Attn: Librarian

No. of Copies	
	NASA Langley Aeronautical Laboratory Langley Field, Virginia
3	Attn: Librarian
1	Attn: C. H. McLellan
1	Attn: J. J. Stack
1	Attn: Adolf Busemann
1	Attn: Comp. Res. Div.
1	Attn: Theoretical Aerodynamics Div.
	NASA Lewis Flight Propulsion Lab. 21000 Brookpark Road Cleveland 11, Ohio
1	Attn: Librarian
1	Attn: Chief, Propulsion Aerodynamics Div.
	NASA 1520 H Street, N. W. Washington 25, D. C.
1	Attn: Chief, Division of Research Information
	Office of the Assistant Secretary of Defense (R & D) Room 3E1065, The Pentagon Washington 25, D. C.
1	Attn: Technical Library
	Research and Development Board Room 3D1041, The Pentagon Washington 25, D. C.
2	Attn: Library
10	ASTIA Arlington Hall Station Arlington 12, Virginia Attn: TIPDR
	Commander, NAMTC Point Mugu, California
1	Attn: Technical Library
	Commanding General Aberdeen Proving Ground, Md.
1	Attn: Technical Info. Br.
1	Attn: Ballistics Res. Lab.

Director of Intelligence
Headquarters, USAF
Washington 25, D. C.
1 Attn: AFOIN-3B

Commander, WADC
Wright-Patterson AF Base
Ohio
2 Attn: WCOSI-3
1 Attn: WCLSW-5
3 Attn: WCRRD

Washington AF Development
Field Office
Room 4549, Munitions Bldg.
Washington 25, D. C.
1 Attn: T. J. Borgstrom

Air Force Ballistic Missile Div.
HG Air Research & Development
Command
P. O. Box 262
Inglewood, California
1 Attn: WDTLAR

Defense Atomic Support Agency
Washington 25, D. C.
1 Attn: Document Library

Commanding General
Arnold Engineering Development
Center
Tullahoma, Tennessee
1 Attn: Technical Library
5 Attn: AEKS

Commanding Officer, DOFL
Washington 25, D. C.
1 Attn: Library
Room 211, Bldg. 92

Commanding General
Army Ballistic Missile Agency
Huntsville, Alabama
1 Attn: ORDAB-DA
1 Attn: Dr. E. Geissler
1 Attn: Mr. T. Reed
1 Attn: Mr. H. Paul
1 Attn: Mr. W. Dahm

Commanding General
Redstone Arsenal
Huntsville, Alabama
1 Attn: Mr. N. Shapiro
ORDDW-MRF

Office, Chief of Ordnance
Department of the Army
Washington 25, D. C.
1 Attn: ORDTU

APL/JHU (C/NOrd 7386)
8621 Georgia Avenue
Silver Spring, Maryland
2 Attn: Tech. Reports Group
1 Attn: Mr. E. Bonney
1 Attn: Mr. D. Fox
1 Attn: Dr. F. Hill

Superintendent
U. S. Naval Postgraduate School
Monterey, California
1 Attn: Tech. Rpts. Section Library

National Bureau of Standards
Washington 25, D. C.
1 Attn: Chief, Fluid Mechanics Section

University of Minnesota
Rosemount Research Laboratories
Rosemount, Minnesota
1 Attn: Technical Library

1 Director
Air University Library
Maxwell AF Base, Alabama

Douglas Aircraft Company, Inc.
Santa Monica Division
3000 Ocean Park Boulevard
Santa Monica, California
1 Attn: Chief Missiles Engineer
1 Attn: Aerodynamics Section

1 CONVAIR
A Division of General Dynamics Corporation
Daingerfield, Texas

CONVAIR Scientific Res. Lab.
5001 Kearney Villa Rd.
San Diego, California
1 Attn: Mr. M. Sibulkin
1 Attn: Asst. to the Dir. of Scientific Research

Republic Aviation Corporation
Farmingdale, New York
1 Attn: Technical Library

Gen. Applied Science Lab., Inc.
Merrick & Stewart Avenues
Westbury, Long Island, N. Y.
1 Attn: Mr. Walter Daskin
1 Attn: Mr. R. W. Byrne

1 CONVAIR
A Division of General Dynamics Corporation
Fort Worth, Texas

United Aircraft Corporation
400 Main Street
East Hartford 8, Connecticut
1 Attn: Chief Librarian
2 Attn: Mr. W. Kuhrt, Research Dept.
1 Attn: Mr. J. G. Lee
1 Attn: Mr. W. E. Powers

Hughes Aircraft Company
Florence Avenue at Teale St.
Culver City, California
1 Attn: Mr. D. H. Johnson R & D Tech. Library

1 McDonnell Aircraft Corporation
P. O. Box 516
St. Louis 3, Missouri

Lockheed Aircraft Corporation
Missile & Space Division
Sunnyvale, California
1 Attn: Dr. L. H. Wilson
4 Attn: Mr. W. E. Brandt
1 Attn: Mr. M. Tucker
1 Attn: Mr. B. W. March
1 Attn: Mr. W. J. Fleming, Jr.

The Martin Company
Baltimore 3, Maryland
1 Attn: Library
1 Attn: Chief Aerodynamicist

North American Aviation, Inc.
Aerophysics Laboratory
Downing, California
1 Attn: Dr. E. R. Van Driest

1 BuWeps Representative
Aerojet-General Corporation
6352 N. Irwindale Avenue
Azusa, California

1 Boeing Airplane Company
Seattle, Washington

RAND Corporation
1700 Main Street
Santa Monica, California
1 Attn: Lib., USAF Project RAND

Arnold Research Organization, Inc.
Tullahoma, Tennessee
1 Attn: Tech. Library
1 Attn: Chief, Propulsion Wind Tunnel
1 Attn: Dr. J. L. Potter

General Electric Company
Missile and Space Vehicles Dept.
3198 Chestnut Street
Philadelphia, Pennsylvania
2 Attn: Larry Chasen Mgr. Library
1 Attn: Mr. R. Kirby
1 Attn: Dr. J. Farber
1 Attn: Dr. G. Sutton
1 Attn: Dr. S. M. Scala
1 Attn: Dr. H. Lew

Eastman Kodak Company
Navy Ordnance Division
50 West Main Street
Rochester 14, New York
2 Attn: W. B. Forman

Reports Distribution Office
Avco-Emerett Res. Laboratory
2385 Revere Beach Parkway
Everett 49, Massachusetts
3 Attn: Dr. J. Ekerman

1 AER, Incorporated
871 East Washington Street
Pasadena, California

Armour Research Foundation
10 West 35th Street
Chicago 16, Illinois
2 Attn: Dept. M

Chance-Vought Aircraft, Inc.
Dallas, Texas
2 Attn: Librarian

Ramo-Woolridge Corporation
Guided Missiles Research Div.
Los Angeles 45, California
1 Attn: Dr. G. Solomon

Cornell Aeronautical Lab., Inc.
4455 Genessee Street
Buffalo 21, New York
1 Attn: Librarian
1 Attn: J. Logan, Jr.

Defense Research Laboratory
The University of Texas
P. O. Box 8029
Austin 12, Texas
1 Attn: Assistant Director

Ohio State University
Columbus 10, Ohio
1 Attn: Security Officer
1 Attn: Aerodynamics Lab.
1 Attn: Mr. J. Lee
1 Attn: Chairman, Dept. of Aeronautical Engin'ing.

CIT
Pasadena, California
1 Attn: Guggenheim Aeronautical Lab., Aeronautics Library
1 Attn: Jet Propulsion Lab.
1 Attn: Dr. H. Liepmann
1 Attn: Dr. L. Lees
1 Attn: Dr. D. Coles
1 Attn: Mr. A. Roshko

Cast Institute of Technology
Cleveland 6, Ohio
1 Attn: G. Kuerti

Massachusetts Institute of
Technology, Cambridge, Mass.
1 Attn: Prof. J. Kaye
1 Attn: Prof. M. Finston
1 Attn: Mr. J. Baron
1 Attn: Mr. M. Sweeney, Jr.

New York University
45 Fourth Avenue
New York 3, New York
1 Attn: Prof. R. Courant
1 Attn: Prof. H. Ludloff

Polytechnic Institute of
Brooklyn
527 Atlantic Avenue
Freeport, New York
1 Attn: Dr. A. Ferri
1 Attn: Dr. M. Bloom
1 Attn: Dr. P. Libby

Brown University
Division of Engineering
Providence, Rhode Island
1 Attn: Prof. R. Probstein
1 Attn: Prof. C. Lin

University of Minnesota
Minneapolis 14, Minnesota
1 Attn: Dr. E. R. G. Eckert
1 Attn: Dr. J. Hartnett
1 Attn: Heat Transfer Lab.
1 Attn: Tech. Library

Rensselaer Polytechnic Institute
Troy, New York
1 Attn: Dept. of Aeronautical
Engineering

Princeton University
James Forrestal Research Center
Gas Dynamics Laboratory
1 Attn: Prof. S. Bogdonoff

Institute for Fluid Dynamics
and Applied Mathematics
University of Maryland
College Park, Maryland
2 Attn: Director
1 Attn: Dr. J. Burgers

University of Michigan
Ann Arbor, Michigan
1 Attn: Dr. A. Kuethe

1 Applied Mathematics and
Statistics Laboratory
Stanford University
Stanford, California

Cornell University
Graduate School of Aero. Engr.
Ithaca, New York
1 Attn: Prof. W. R. Sears

The Johns Hopkins University
Charles and 34th Streets
Baltimore, Maryland
1 Attn: Dr. F. H. Clauser

University of California
Berkeley 4, California
1 Attn: C. Maslach
1 Attn: Dr. S. Schaaf

1 Mr. J. Lukasiewicz
Chief, Gas Dynamics Facility
ARO, Incorporated
Tullahoma, Tennessee

1 Mr. Rex Monaghan
RAE, Farnsborough, England
c/o British Joint Services
Mission
Attn: Aircraft Branch
P. O. Box 680
Benjamin Franklin Station
Washington, D. C.

Naval Ordnance Laboratory, White Oak, Md.
(NAVORD report 4516)
DYNAMIC AND STATIC STABILITY MEASUREMENTS OF THE BASIC FINNER AT SUPERSONIC SPEEDS, by Irving Shantz and Robert T. Groves. 14 Jan. 1960. 10p. illus., charts, tables, diagrs. (Aerodynamics research report 390). Project 803-717/73001/03073. UNCLASSIFIED

Dynamic stability data in the form of damping force and moment coefficients were obtained in the NOL supersonic tunnel no. 1. These measurements were made in the Mach number range 1.58 through 3.24. Static stability data in the form of normal force and pitching moment coefficients were determined in the Mach number range 1.58 through 3.86. Both dynamic and static stability coefficients are compared with free flight results obtained in the NOL and BRL ballistics firing ranges.

1. Bodies - Aerodynamics
2. Bodies - Supersonic speeds
3. Bodies - Stability
I. Title
II. Shantz, Irving
III. Groves, Robert T., jt. author
IV. Series
V. Project

Naval Ordnance Laboratory, White Oak, Md.
(NAVORD report 4516)
DYNAMIC AND STATIC STABILITY MEASUREMENTS OF THE BASIC FINNER AT SUPERSONIC SPEEDS, by Irving Shantz and Robert T. Groves. 14 Jan. 1960. 10p. illus., charts, tables, diagrs. (Aerodynamics research report 390). Project 803-717/73001/03073. UNCLASSIFIED

Dynamic stability data in the form of damping force and moment coefficients were obtained in the NOL supersonic tunnel no. 1. These measurements were made in the Mach number range 1.58 through 3.24. Static stability data in the form of normal force and pitching moment coefficients were determined in the Mach number range 1.58 through 3.86. Both dynamic and static stability coefficients are compared with free flight results obtained in the NOL and BRL ballistics firing ranges.

1. Bodies - Aerodynamics
2. Bodies - Supersonic speeds
3. Bodies - Stability
I. Title
II. Shantz, Irving
III. Groves, Robert T., jt. author
IV. Series
V. Project

Naval Ordnance Laboratory, White Oak, Md.
(NAVORD report 4516)
DYNAMIC AND STATIC STABILITY MEASUREMENTS OF THE BASIC FINNER AT SUPERSONIC SPEEDS, by Irving Shantz and Robert T. Groves. 14 Jan. 1960. 10p. illus., charts, tables, diagrs. (Aerodynamics research report 390). Project 803-717/73001/03073. UNCLASSIFIED

Dynamic stability data in the form of damping force and moment coefficients were obtained in the NOL supersonic tunnel no. 1. These measurements were made in the Mach number range 1.58 through 3.24. Static stability data in the form of normal force and pitching moment coefficients were determined in the Mach number range 1.58 through 3.86. Both dynamic and static stability coefficients are compared with free flight results obtained in the NOL and BRL ballistics firing ranges.

1. Bodies - Aerodynamics
2. Bodies - Supersonic speeds
3. Bodies - Stability
I. Title
II. Shantz, Irving
III. Groves, Robert T., jt. author
IV. Series
V. Project